New Phytologist

The *MTP1* promoters from *Arabidopsis halleri* reveal *cis*-regulating elements for the evolution of metal tolerance

Elisa Fasani[1], Giovanni DalCorso[1], Claudio Varotto[2], Mingai Li[2], Giovanna Visioli[3], Monica Mattarozzi[3] and Antonella Furini[1]

[1]Department of Biotechnology, University of Verona, Strada Le Grazie 15, Verona 37134, Italy; [2]Department of Biodiversity and Molecular Ecology, Research and Innovation Centre, Fondazione Edmund Mach, Via E. Mach 1, San Michele all'Adige (TN) 38010, Italy; [3]Department of Chemistry, Life Sciences and Environmental Sustainability, Parco Area delle Scienze, 11/A, Parma 43124, Italy

Author for correspondence:
Antonella Furini
Tel: +39 045 802 7950
Email: antonella.furini@univr.it

Received: *16 December 2016*
Accepted: *14 February 2017*

New Phytologist (2017) **214:** 1614–1630
doi: 10.1111/nph.14529

Key words: *Arabidopsis halleri*, *cis*-acting regulatory elements, metal hyperaccumulation/tolerance, *MTP1* promoter, trichomes, zinc (Zn) tolerance.

Summary

- In the hyperaccumulator *Arabidopsis halleri*, the zinc (Zn) vacuolar transporter MTP1 is a key component of hypertolerance. Because protein sequences and functions are highly conserved between *A. halleri* and *Arabidopsis thaliana*, Zn tolerance in *A. halleri* may reflect the constitutively higher *MTP1* expression compared with *A. thaliana*, based on copy number expansion and different *cis* regulation.
- Three *MTP1* promoters were characterized in *A. halleri* ecotype I16. The comparison with the *A. thaliana MTP1* promoter revealed different expression profiles correlated with specific *cis*-acting regulatory elements.
- The *MTP1* 5′ untranslated region, highly conserved among *A. thaliana*, *Arabidopsis lyrata* and *A. halleri*, contains a dimer of MYB-binding motifs in the *A. halleri* promoters absent in the *A. thaliana* and *A. lyrata* sequences. Site-directed mutagenesis of these motifs revealed their role for expression in trichomes. *A. thaliana mtp1* transgenic lines expressing *AtMTP1* controlled by the native *A. halleri* promoter were more Zn-tolerant than lines carrying mutations on MYB-binding motifs. Differences in Zn tolerance were associated with different distribution of Zn among plant organs and in trichomes.
- The different *cis*-acting elements in the *MTP1* promoters of *A. halleri*, particularly the MYB-binding sites, are probably involved in the evolution of Zn tolerance.

Introduction

Plants have evolved different adaptive strategies to extreme environmental conditions. Metal hypertolerance and hyperaccumulation (i.e. the ability to tolerate exceptionally high concentrations of metals in soil and to accumulate them in the above-ground tissues, respectively; Baker, 2002; Krämer, 2010), are particularly interesting because understanding the combination of underlying mechanisms provides useful insights into the metal homeostasis network and the evolution of adaptive traits. Furthermore, such knowledge could be used to develop phytoremediation and biofortification technologies (Verbruggen *et al.*, 2013). Recent efforts to understand the genetic mechanisms of metal hyperaccumulation have focused mostly on the Brassicaceae family, in which the trait has evolved independently several times (Krämer, 2010). The zinc (Zn) and cadmium (Cd) hyperaccumulators *Arabidopsis halleri* and *Noccaea caerulescens* have attracted the most interest as a result of their close phylogenetic relationship with *Arabidopsis thaliana*, which provides a deeper insight into the molecular basis of hyperaccumulation.

Although it is evident that hyperaccumulation requires tolerance to high concentrations of metals in leaves, the two characters are mostly genetically independent, as indicated by the quantitative trait locus (QTL) analysis on F_2 populations derived from interspecific crosses of *A. halleri* and the closely related *Arabidopsis lyrata* ssp. *petraea*, which is both nontolerant and a nonaccumulator (Macnair *et al.*, 1999; Bert *et al.*, 2003). Indeed, Zn tolerance has been found as associated with three major QTLs in a metallicolous population of *A. halleri*: the most promising candidates resulting from this analysis were the *loci* coding for the metal transporters AhHMA4, AhMTP1-A1/A2 and AhMTP1-B (Willems *et al.*, 2007). The QTL containing *AhHMA4*, partially accounting for Zn tolerance, overlaps with QTLs responsible for Zn accumulation in both low and high Zn pollution levels (Frérot *et al.*, 2010), as well as for Cd tolerance and accumulation (Courbot *et al.*, 2007; Willems *et al.*, 2010), suggesting a partial pleiotropic control of these traits (Verbruggen *et al.*, 2009).

At the molecular level, both hypertolerance and hyperaccumulation reflect the up-regulation of several classes of metal transporters, chelators and proteins involved in stress responses. Genes into these categories are expressed at higher levels in hyperaccumulator species than in corresponding nonmetallophyte species, as highlighted by both transcriptomic analysis (Becher *et al.*, 2004; Weber *et al.*, 2004; Hammond *et al.*, 2006; van de Mortel

et al., 2006) and proteomic comparisons (Tuomainen *et al.*, 2010; Visioli *et al.*, 2010). The up-regulation of some key components reflects the synergistic action of copy number expansion and differential transcriptional *cis*-regulation, as observed for genes such as *HMA4* (Hanikenne *et al.*, 2008; Nouet *et al.*, 2015) and *MTP1* (Shahzad *et al.*, 2010). Regulation at the post-translational level has also been reported (Elbaz *et al.*, 2006).

Many of the genes involved in metal hypertolerance/hyperaccumulation encode different families of transporters that participate in root uptake, translocation and compartmentalization, mainly into the vacuole (Krämer *et al.*, 2007). The cation diffusion facilitator (CDF) transporter family is particularly important in metal hyperaccumulation. CDF proteins are ubiquitous in both prokaryotes and eukaryotes (Nies & Silver, 1995), and they transport metals against a gradient using a metal/H^+ antiport strategy (Guffanti *et al.*, 2002). In plants, CDF transporters are known as the metal tolerance protein (MTP) family; MTP1 has attracted particular attention as a result of the strong evidence supporting its role in Zn tolerance. In *A. thaliana*, MTP1 shows specificity for Zn (Bloß *et al.*, 2002), and is localized in the tonoplast (Desbrosses-Fonrouge *et al.*, 2005). Overexpression in *A. thaliana* confers increased Zn tolerance and facilitates Zn accumulation reflecting enhanced metal detoxification by vacuolar sequestration (van der Zaal *et al.*, 1999). *MTP1* is expressed at higher levels in the hyperaccumulators *A. halleri* (Becher *et al.*, 2004; Dräger *et al.*, 2004; Talke *et al.*, 2006), *N. caerulescens* (Assunção *et al.*, 2001; van de Mortel *et al.*, 2006) and *Noccaea goesingense* (Persans *et al.*, 2001) than in related non-metallophyte species. In a metallicolous population of *A. halleri* autochthonous in Auby (northern France), *MTP1* cosegregates with QTLs for Zn hypertolerance and has undergone copy number expansion relative to its orthologs in congeneric nonaccumulators (Dräger *et al.*, 2004; Willems *et al.*, 2007).

The analysis of the Auby population revealed five *MTP1* loci named *AhMTP1-A1*, *AhMTP1-A2*, *AhMTP1-B*, *AhMTP1-C* and *AhMTP1-D* (Dräger *et al.*, 2004; Shahzad *et al.*, 2010). These five paralogs encode proteins with 97.5% mean intraspecific identity and 91–93% identity with orthologs from *A. thaliana* and *A. lyrata*. All five copies are expressed constitutively, but the *AhMTP1-A1*/*A2*/*B* transcripts are three orders of magnitude more abundant than those of *AhMTP1-C*/*D* (Shahzad *et al.*, 2010). However, in a nonmetallicolous Slovakian population, *AhMTP1* is present in single copy and is not associated with the single QTL found for Zn tolerance, which includes *AhHMA4*. This evidence suggests that the constitutive Zn tolerance may be linked to the presence of AhHMA4 in all *A. halleri* populations, whereas AhMTP1 may be responsible for the additional increase in tolerance observed specifically in the metallicolous ones (Meyer *et al.*, 2016).

Here we analyzed the *MTP1* loci in the metallicolous *A. halleri* population I16, collected in Val del Riso (northern Italy), a calamine valley highly contaminated with Zn, Cd and Pb (Meyer *et al.*, 2015). This population belongs to the southern phylogeographic group of *A. halleri* and therefore provides interesting material for comparison with populations from the northern genetic background as Auby (Pauwels *et al.*, 2012). Promoters corresponding to four different loci were identified, three of which could not be assigned to *MTP1* promoter A, B and C copies identified in the Auby population: the three novel sequences, pAhMTP1-α, pAhMTP1-β, and pAhMTP1-γ, share high homology in the first 800 bp upstream of the start codon with the promoter sequences of the Auby population and diverge in the upstream region, whereas pAhMTP1-D is conserved in both populations (and therefore the same nomenclature has been maintained).

Most importantly, the comparison of these promoter sequences with their *A. thaliana* and *A. lyrata* counterparts revealed MYB-binding sites that are present in *A. halleri* but not *A. thaliana* or *A. lyrata*. These MYB sites are required for *MTP1* expression in the trichomes and support the hypertolerance phenotype of *A. halleri*.

Materials and Methods

Plant material and growth conditions

The following Brassicaceae species were used for promoter analysis: *Arabidopsis halleri* (L.) O'Kane & Al-Shehbaz population I16 (Val del Riso, northern Italy, 45°51′34.40 N 9°52′34.94 E; Meyer *et al.*, 2015); *Noccaea praecox* (Wuljen) F.K.Mey., *Cardamine resedifolia* L., *Thlaspi arvense* L., *Cochlearia officinalis* L., *Sisymbrium officinale* (L.) Scop. and *Descurainia sophia* (L.) Webb ex Prantl (wild populations from Trentino, northern Italy); and *Noccaea caerulescens* (J.Presl & C.Presl) F.K.Mey. ecotype Ganges (St Laurent le Minier, southern France; Lombi *et al.*, 2002). Promoter sequences from *Arabidopsis thaliana* (L.) Heynh. accession Columbia (Col-0) and *Arabidopsis lyrata* (L.) O'Kane & Al-Shehbaz were obtained from the Arabidopsis Information Resource (TAIR) (http://www.arabidopsis.org; Lamesch *et al.*, 2012). *Arabidopsis thaliana* Col-0 and *mtp1* mutant were used for the stable transformation (see Supporting Information Methods S1); the *mtp1* homozygous mutant (SALK_204398C) was obtained from NASC (http://arabidopsis.info; Scholl *et al.*, 2000).

Plants were cultivated in soil in the glasshouse, with a 16 h photoperiod at 23°C (standard growth conditions). For *in vitro* cultivation, seeds were sterilized with 70% ethanol for 1 min, and then with 10% sodium hypochlorite containing 0.03% Triton X-100 for 15 min, before being rinsed three times with sterile water. Sterile seeds were sown on solid MS medium (Murashige & Skoog, 1962) supplemented with 30 g l^{-1} sucrose and vernalized for 2 d at 4°C. Plants were maintained *in vitro* with a 16 h photoperiod at 23°C.

Promoter isolation and sequencing

Genomic DNA was extracted from the species listed earlier using the Qiagen Genomic DNA Extraction Kit. The promoter fragments were obtained by using the GenomeWalker Universal Kit (Clontech Laboratories Inc., Mountain View, CA, USA) according to the manufacturer's instructions, combining the *MTP1* coding sequence-specific primer MTP1_1 and its nested primer MTP1_2 (Table 1). *Taq* DNA polymerase was used to add

Table 1 Primer sequences

Target sequence	Primer sequence
MTP1 promoter cloning by Genome Walking	MTP1_1: CAACGAAATGAGCTGGATAGACACAAG MTP1_2: GATAGCAAAGGCAGCAACGTCAGAGA
GUS	Fw: GGTACCATGGTCCGTCCTGTAGAAACC Rev: CTCGAGATTATTGTTTGCCTCCCTGCTG
CDS of *Arabidopsis thaliana MTP1* - *AtMTP1* (At2g46800)	Fw: GGTACCATGGAGTCTTCAAGTCCCCA Rev: CTCGAGTTAGCGCTCGATTTGTATCG
A. thaliana MTP1 promoter pAtMTP1	Fw: CCCGGGTGTTCGAAGTTTGGAAAGT Rev: GGTACCCTGCATAAGAAAAAAAATAGAAGA
Arabidopsis halleri MTP1 promoters pAhMTP1-A1 and -A2	Fw1 (−1205 bp): ATAAGTTCAACATGTTTTCACGTA Fw2 (−947 bp): TAATGTTTTAATGTTTTGACCAATG Rev: CTGCATAGAAAAAGAAGAAAGTTA
A. halleri MTP1 promoter pAhMTP1-B	Fw1 (−1195 bp): CCTCATGTTCCTCATCATTCC Fw2 (−993 bp): GCCCTCATTGTAACTAGTCGT Rev: CTGCATAGAAAAAGAAGAAAGTTA
A. halleri MTP1 promoters pAhMTP1-C and pAhMTP1-D	Fw1 (−1335 bp): GATGGTGTAGTTTTGCCCGC Fw2 (−1060 bp): ATCGGGGACAAGATCTGGAG Rev: CTGCATAGAAAAAGAAGAAAGTTA
A. halleri MTP1 entire promoters pAhMTP1-α, -β and -γ	Fw: CCCGGGTCTTATCCGTGCTAGTAGTTG Rev: GGTACCCTGCATAGAAAAAGAAGAAAGTTA
A. halleri MTP1 truncated promoter Δ810	Fw: CCCGGGTCATTTTGCTAAACGGCTTCTGC Rev: GGTACCCTGCATAGAAAAAGAAGAAAGTTA
A. halleri MTP1 truncated promoter Δ362	Fw: CCCGGGTTGGTAACGCTCTTGAATCTGTT Rev: GGTACCCTGCATAGAAAAAGAAGAAAGTTA
Mutagenesis of −125 bp position in *A. halleri MTP1* promoter	GAAAACTCTTGTGCTTCTATTGAATTGG AAGCACAAGAGTTTTCTGAACTTGG
Mutagenesis of −155 bp position in *A. halleri MTP1* promoter	CTTTTTTGTTGAAACAGTTTACCAAG TGTTTCAACAAAAAAGAAAGCAAATTTATC
Mutagenesis of −303 bp position in *A. halleri MTP1* promoter	ATCAAGGGGGGGGGAATACCGATTCAAG TATTGCCCCCCCCCTTGATGATTATTATATG
Mutagenesis of −400 bp position in *A. halleri MTP1* promoter	AACCCAGGGGGGGGGAAACGTGGGGCTGG ACGTTTCCCCCCCCCTGGGTTTTCTTCAAAATC
AhMTP1-α for real-time RT-PCR on *A. halleri MTP1* 5′UTR	Fw: GGGCCAGCCCCAGGGTC Rev: AAGTGTGAAGAATCTACAAACC
AhMTP1-β for real-time RT-PCR on *A. halleri MTP1* 5′UTR	Fw: GGGCCAGCCCCAGGGTA Rev: AAGTGTGAAGAATCTACAAACC
AhMTP1-γ for real-time RT-PCR on *A. halleri MTP1* 5′UTR	Fw: ATACATGTCTTTGTCCTTTGAG Rev: CAGAACTCGAAATCAACAAACG
AhMTP1-D for real-time RT-PCR on *A. halleri MTP1* 5′UTR	Fw: CTCGCTTAGGGGCCCAGC Rev: CTAAAATATCGATTCAAGTTTGAA
GUS for real-time RT-PCR	Fw: TACACCGACATGTGGAGTGA Rev: CCATACCTGTTCACCGACG
MTP1 for real-time RT-PCR	Fw: GGAGAGTACACCCAGAGAGAT Rev: GCCCAAATGTGAAGCTCATGAA
β-*actin* (At5g09810)	Fw: GAACTACGAGCTACCTGATG Rev: CTTCCATTCCGATGAGCGAT
Ubiquitin 10 (At4g05320)	Fw: AGGACAAGGAAGGTATTCCTC Rev: CTCCTTCTGGATGTTGTAGTC

The underlined nucleotides indicate the restriction sites introduced by PCR. The underlined italics nucleotides indicate the mutagenized sequences. RT-PCR, reverse transcription polymerase chain reaction.

adenylate tails to the amplified promoter fragments for cloning in the pGEM-T vector (Promega). The positive clones were purified and sequenced with a 96-capillary 3730xl DNA Analyzer (Applied Biosystems, Foster City, CA, USA). Promoter analysis was performed as described in Methods S2.

Expression analysis of *AhMTP1*-α/β/γ and D in *A. halleri* I16

Total RNA was extracted with TRIzol Reagent (Thermo Fisher Scientific, Waltham, MA, USA); three pools from leaves of 3-wk-old plants grown in control conditions were used as biological replicates. After DNase treatment, first-strand cDNA was synthesized using the Superscript III Reverse Transcriptase Kit (Thermo Fisher Scientific). Real-time reverse transcription polymerase chain reaction (RT-PCR) was performed with a StepOnePlus Real-Time PCR System (Applied Biosystems) using KAPA SYBR FAST ABI Prism 2X qPCR Master Mix (Kapa Biosystems, Wilmington, MA, USA). Each reaction (40 amplification cycles) was carried out in triplicate and melting curve analysis was used to confirm the amplification of specific targets. Primers

for this analysis were designed on discriminating sequences of the 5′ untranslated region (UTR) and are reported in Table 1. Data were normalized using the two endogenous reference genes β-*actin* (At5g09810) and *ubiquitin 10* (At4g05320) and analyzed using the $2^{-\Delta\Delta CT}$ method (Livak & Schmittgen, 2001). The amplification efficiency of each primer pair (*c.* 2) was calculated using LinRegPCR v.7.5 software (Ramakers *et al.*, 2003).

Cloning and DNA manipulation

MTP1 promoter sequences were amplified using genomic DNA templates from *A. thaliana* (for pAtMTP1) and *A. halleri* population I16 (for pAhMTP1-α/β/γ and truncated forms Δ810 and Δ362). A PCR approach was followed in order to verify the existence in the I16 population of the AhMTP1-A1/A2/B/C/D promoters, found in the *A. halleri* collected in Auby (Shahzad *et al.*, 2010). These reactions were performed with different primers designed on the available sequences corresponding to the four different copies present in Auby genotype (Table 1); different PCR conditions (both magnesium (Mg) stringency and annealing temperatures) were tested.

Platinum *Pfx* DNA polymerase (Thermo Fisher Scientific) was used according to the manufacturer's instructions with the primers listed in Table 1. For the generation of the mut303/400, mut155 and mut125/155 sequences, site-directed mutagenesis was performed on the pGEM-pAhMTP1-γ plasmid using *Pfu* polymerase (Promega) and the mutagenic primers listed in Table 1 (19 cycles of 95°C for 30 s, 55°C for 1 min and 68°C for 9 min). The parental DNA was digested with *Dpn*I (Promega) and the mutagenesis product was used to transform *Escherichia coli* strain DH5α.

The β-glucuronidase (*GUS*) gene was amplified from the vector pENTR-*GUS* (Thermo Fisher Scientific). The *AtMTP1* coding sequence was amplified from *A. thaliana* genomic DNA using the primers listed in Table 1 and cloned in the pGEM-T easy vector (Promega). The sequences pAtMTP1, pAhMTP1-α/β/γ, Δ810, Δ362, mut303/400, mut155 and mut125/155 were digested using the enzymes *Sph*I and *Kpn*I and fused to the *GUS* gene. The sequences pAhMTP1-γ and mut125/155 were also fused to the *AtMTP1* coding sequence. All cassettes were cloned in vector pMD1 (Das *et al.*, 2001) which was deprived of the CaMV 35S promoter by cutting with *Hind*III and *Xho*I.

Analysis of GUS expression

For the histochemical GUS assay, plant tissues (six 10-d-old plantlets and leaves of 3-wk-old plants for three lines for each construct) were incubated overnight at 37°C in GUS reaction buffer (100 mM sodium phosphate, pH 7.0, 1 mM EDTA, pH 8.0, 2 mM potassium ferrocyanide, 2 mM potassium ferricyanide, 1% Triton X-100, 500 mg l^{-1} 5-bromo-4-chloro-3-indolyl β-D-glucuronide in dimethylformamide). Chlorophylls were removed by incubating the tissues in 70% ethanol at 70°C. Plants were examined using a Zoom stereomicroscope AZ100 (Nikon, Tokyo, Japan) and a Leica DM RB microscope (Leica Microsystems GmbH, Wetzlar, Germany).

Fluorimetric GUS assays were carried on three pools of leaves collected from five plants for each transgenic line (three lines were considered for each constructs described). Plants were 3-wk-old and grown under standard growth conditions. GUS activity was detected as described by Cervera (2004). Fluorimetric measurements were performed using a Jasco FP-8200 spectrofluorometer (Jasco Inc., Easton, MD, USA) at an excitation wavelength of 365 nm and an emission wavelength of 455 nm.

Analysis of Zn tolerance

Tolerance to Zn was tested *in vitro* on *A. thaliana* plants transformed with the empty pMD1 vector (control) and *mtp1* mutant plants, as references, and on three homozygous single-copy lines for both the pAhMTP1-γ*::AtMTP1* and mut125/155*::AtMTP1* constructs; each line displayed similar expression levels in real-time RT-PCR analysis (Methods S3). Eighteen plants representing each line were considered under each experimental condition. One-week-old plantlets were grown for 8 d in Gelrite-solidified MS medium containing different $ZnSO_4$ concentrations: 30 μM ($ZnSO_4$ concentration in standard MS medium), 300 and 500 μM. Zn tolerance was evaluated in terms of root length, biomass and Chl content. Chlorophylls were extracted in buffered 80% aqueous acetone and the total Chl content was measured as described by Porra *et al.* (1989).

Analysis of Zn accumulation

mtp1 plants transformed with the pAhMTP1-γ*::AtMTP1* and the mut125/155*::AtMTP1* constructs, as well as control plants, were germinated in solid MS medium and then transferred in hydroponic culture in Hoagland solution (Hoagland & Arnon, 1950). Three-week-old plants were grown in 0.7 and 25 μM $ZnSO_4$ for 7 d, where 0.7 μM is the $ZnSO_4$ concentration in standard Hoagland solution. Leaves and roots were oven-dried separately at 60°C and subjected to microwave-assisted acid digestion (EPA 3052, 1996). The Zn content was determined by inductively coupled plasma MS (EPA 3051A 2007 and EPA 6010C 2007).

Environmental scanning electron microscopy coupled with energy-dispersive X-ray spectroscopy (ESEM-EDS)

Leaves from 3-wk-old plants grown in 25 μM $ZnSO_4$ for 7 d were analyzed for Zn accumulation in single trichomes. Three biological replicates were analyzed for each *A. thaliana* line, two leaves for each line and 10 trichomes for each leaf. All experiments were conducted using an ESEM instrument Quanta 250 FEG (FEI, Hillsboro, OR, USA) equipped with an energy-dispersive spectrometer (EDS) for X-ray microanalysis (Bruker Nano GmbH, Berlin, Germany), operating in wet mode. The EDS has a QUANTAX XFlash 6|30 detector with energy resolution ≤126 eV full width at half maximum at Mnkα. For further details on the analysis, see Methods S4.

Statistical analysis

Statistical significance of the data was evaluated by Welch's ANOVA, followed by a Games–Howell *post hoc* test, according to McDonald (2014). In histograms reported in the figures, error bars correspond to SD, and data with nonsignificant differences ($P > 0.05$) are indicated with the same letter.

Results

Amplification of *MTP1* promoter sequences from *A. halleri* I16

An *MTP1* promoter sequence (1194 bp) was isolated by genome walking from *A. halleri* population I16 and was used to design specific primers for the amplification of further *MTP1* promoter sequences using the I16 genomic DNA as a template. PCR amplification yielded three amplicons (1904, 1698 and 1194 bp) representing different promoter copies designated as α, β and γ, respectively. The γ variant corresponded to the sequence identified by genome walking.

The aligned α, β and γ sequences shared high levels of identity, particularly in the distal and proximal regions (96.8% and 90.2%, respectively). Sequence divergence in the proximal region primarily reflected the presence of a 63 bp insertion in sequences α and β (light blue box in Fig. 1a; Fig. S1). The comparison of the α, β and γ sequences with the five paralogs in the Auby population and the *MTP1* promoters from *A. thaliana* and *A. lyrata* revealed high conservation in the proximal 800 bp (Fig. 1a). The pAhMTP1-γ and pAhMTP1-A1/A2/B/C/D sequences shared > 93% nucleotide identity (Table S1), suggesting that the γ promoter is probably the nearest to the parental sequence from which sequences α and β evolved in the I16 population, as indicated by the phylogenetic tree (Fig. 1b).

Primers based on the promoters of the *AhMTP1-A1/A2/B/C/D* loci of the Auby population were used to amplify *A. halleri* I16 genomic DNA to determine whether these sequences are also present in the I16 genome. A PCR product was obtained for the D copy and the sequence was included in the alignment in Fig. S1. No amplification resulted for pAhMTP1-A/B/C.

Real-time RT-PCR confirms that *AhMTP1-α/β/γ/D* are expressed in *A. halleri* I16, with *AhMTP1-γ* and *AhMTP1-D* having the lowest and highest expression levels, respectively (Fig. S2).

Expression profiles conferred by the *A. thaliana* and *A. halleri MTP1* promoters

The spatial *MTP1* expression profiles conferred by the α, β and γ promoter sequences identified in *A. halleri* I16 and a 2000 bp control sequence amplified from the *A. thaliana MTP1* promoter (pAtMTP1) were determined by GUS assay. Under standard growth conditions, *GUS* expression driven by the *A. thaliana* promoter was weak and localized in the roots, hydathodes, leaf vascular system, guard cells and inflorescence, as previously reported (Desbrosses-Fonrouge *et al.*, 2005; Kawachi *et al.*, 2009). The pAhMTP1-α/β/γ promoters conferred identical *GUS* expression profiles, with intense GUS staining in the shoots and roots, also observed in floral organs, siliques and in the trichomes (Fig. 2a). Quantitative analysis of *GUS* expression confirmed that the pAhMTP1-α/β/γ promoters are two orders of magnitude stronger than the pAtMTP1 promoter, and approximately one order of magnitude stronger than the constitutive 35S CaMV promoter. Among the *AhMTP1* promoters, the α and β sequences showed comparable expression levels, whereas a lower level was observed for the γ promoter (Fig. 2b,c).

Expression profiles conferred by truncated *A. halleri MTP1* promoters

The pAhMTP1-γ promoter was used for the generation of truncated promoter forms in order to define regulatory regions essential for *MTP1* expression in *A. halleri*. A 810-bp-long promoter (Δ810) included the entire proximal region of pAhMTP1, highly conserved among the *A. halleri MTP1* promoter sequences, while the shortest truncated form (Δ362) includes part of the *MTP1* 5′UTR (Fig. 3a). Expression pattern and levels for the Δ810 promoter are approximately the same as in the pAhMTP1-γ entire promoter (Fig. 3b,c). Interestingly, *GUS* expression was completely abolished in the shoots of the Δ362*::GUS* plants but weak GUS staining was observed in the roots (Fig. 3b).

Identification of *cis*-acting elements in the *A. thaliana*, *A. lyrata* and *A. halleri MTP1* promoters

pAhMTP1-γ, *A. thaliana* and *A. lyrata MTP1* promoter sequences were analyzed using the Signal Scan Search tool on the PLACE database to identify annotated *cis*-acting elements. The complete list of the identified motifs is reported in Table S2. No TATA-box was found in any of the promoters, but an initiator element (*Inr*) was found 60, 55 and 54 bp downstream of the putative transcriptional start site in the *A. thaliana*, *A. lyrata* and *A. halleri* promoters, respectively.

PLACE analysis highlighted the presence of several *cis*-acting elements involved in cell/tissue-specific expression. Dof-binding motifs that confer guard cell-specific expression (Plesch *et al.*, 2001) were found in all promoters; one tandem repeat is present in the pAhMTP1-γ sequence, whereas the *A. thaliana* and *A. lyrata* sequences contain five and four tandem repeats, respectively. Some root-specific motifs were also found in all promoters, such as ATATT motifs that possibly drive gene expression in the vasculature (Elmayan & Tepfer, 1995), and *telo*-box motifs that are reported as necessary for expression in root primordia (Tremousaygue *et al.*, 1999; Manevski *et al.*, 2000). Root hair-specific *cis*-acting elements (Kim *et al.*, 2006; Won *et al.*, 2009) were found only in pAtMTP1 and pAhMTP1-γ (Table S2).

Three *telo*-box sequences were found in the *A. thaliana* and *A. lyrata MTP1* promoters, whereas two were found in all *MTP1* promoters in both the I16 and Auby populations (red bars in Fig. 1a). Despite the presence of the 63 bp insertion at position −340 bp in the pAhMTP1-α/β promoters, there was no relevant variation in the spacing between the two motifs in any of the

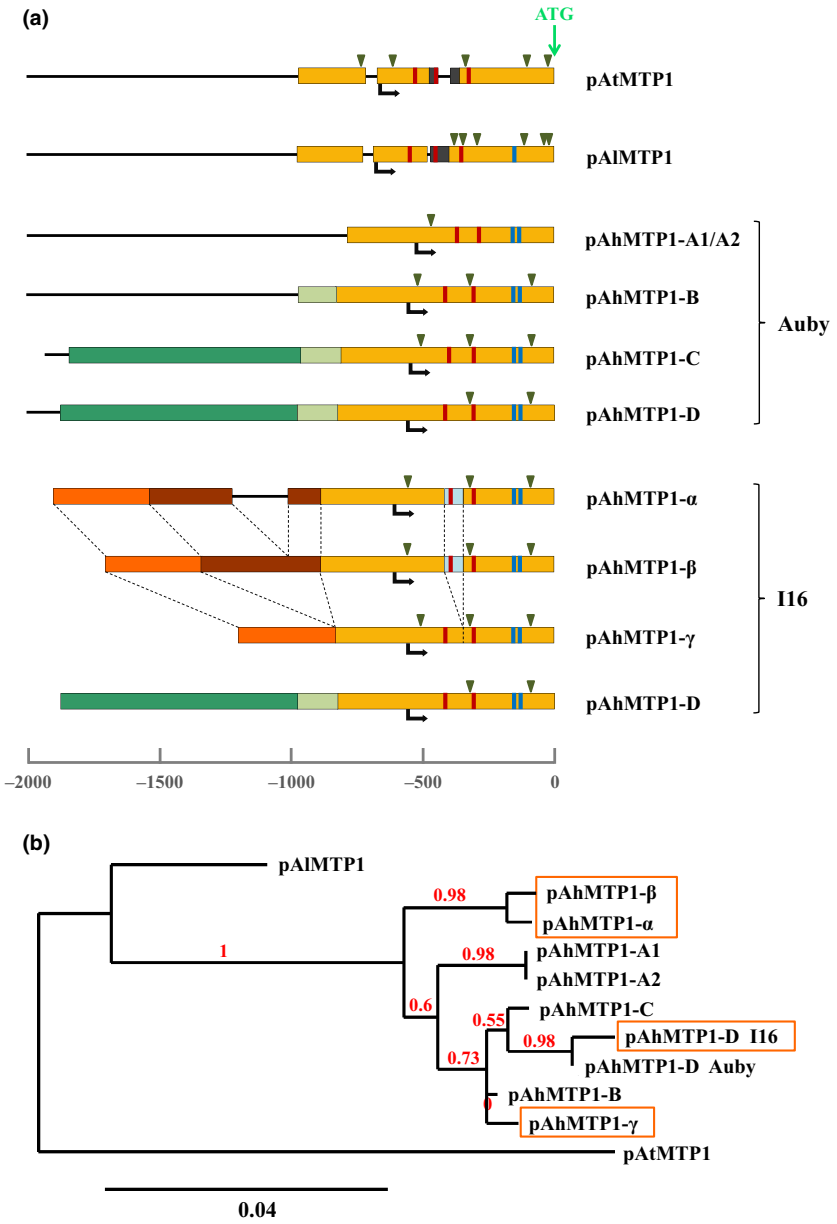

Fig. 1 Homology analysis of the *MTP1* promoters of *Arabidopsis thaliana* (pAtMTP1), *Arabidopsis lyrata* (pAlMTP1) and *Arabidopsis halleri* populations Auby (pAhMTP1-A/B/C/D) and I16 (pAhMTP1-α/β/γ/*D*). GenBank accession numbers for the *MTP1* promoters from *A. halleri* I16 are listed in parentheses as follows: pAhMTP1-α (KU535633); pAhMTP1-β (KU535634); pAhMTP1-γ (KU535635). (a) Schematic representation of the *MTP1* promoters based on multiple alignments. Boxes with the same color indicate highly conserved regions (sequence identity > 80%). Putative transcriptional and translational start sites are indicated by black arrows under the bars and ATG, respectively. Small triangles above the promoter representations indicate short insertions (10–20 bp). The positions of *telo*-boxes and MYB-binding sites in each promoter are indicated by red and blue bars, respectively. (b) Phylogenetic tree of the *MTP1* promoters of the *Arabidopsis* species considered, generated by phylogeny. The sequences identified in the I16 population of *A. halleri* are highlighted in orange boxes. Red numbers over the branches are the branch support values. The black bar under the tree indicates branch length.

promoters. Indeed, the distal motif is located within the insertion in sequences α and β but upstream of the insertion site in sequence γ and all the Auby promoters (Fig. 1a). The activity of *telo*-boxes has been reported to require other *cis*-acting elements, such as the *tef*-box, *trap-40* elements and site II motifs (Tremousaygue *et al.*, 1999; Manevski *et al.*, 2000; Gaspin *et al.*, 2010). The *MTP1* promoters were therefore screened for these motifs but none were present.

Notably, a tandem repeat of MYB-binding elements (CTGTTG; blue bars in Fig. 1a) with a putative role in trichome-specific gene expression (Wang *et al.*, 2002) was identified in all the *A. halleri MTP1* promoter sequences. The motifs are located in the 5′UTR 125 and 155 bp upstream of the start codon. Despite the high degree of conservation among the *A. thaliana*, *A. lyrata* and *A. halleri MTP1* promoters in the 5′UTR, the MYB-binding elements were not found in pAtMTP1 as a result of single point mutations, whereas only one site is conserved in pAlMTP1 (Fig. 4). The promoters of several *A. thaliana* genes involved in metal tolerance and accumulation (Table S3) were also screened for this motif but no paired MYB-binding sites were found in the 5′UTRs of any of these genes.

Site-directed mutagenesis of *telo*-boxes

The *telo*-box motifs (TTAGGGTT) were selected for further analysis as a result of their conservation in both sequence and position among the *A. halleri*, *A. thaliana* and *A. lyrata* promoters (Fig. 1a) and their putative role for expression in root primordia. Double site-directed mutagenesis on the pAhMTP1-γ promoter replaced the TTAGGGTT sequences at position −303 and −400 bp with a C_8 substitute to preserve the relative spacing of

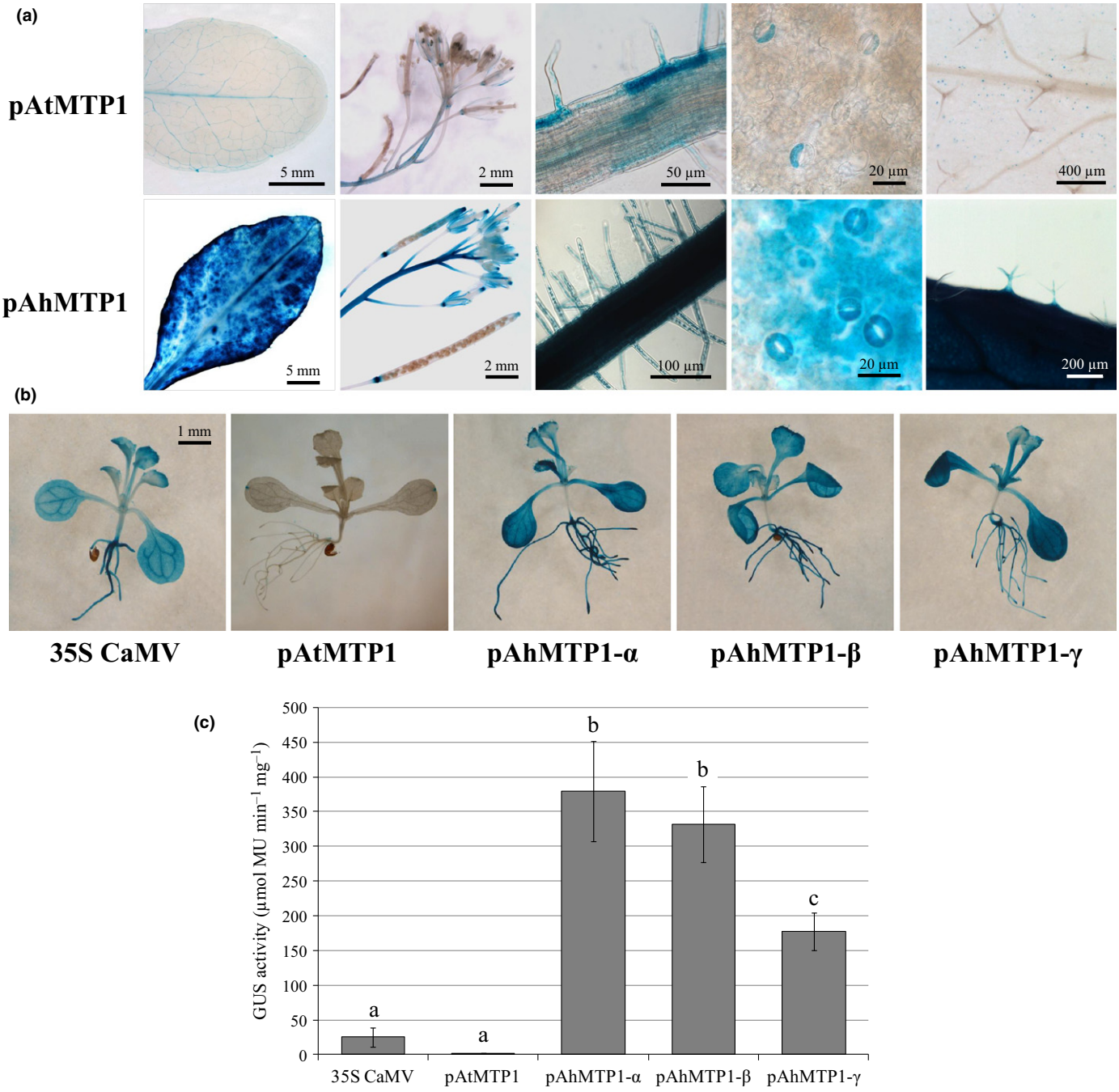

Fig. 2 β-Glucuronidase (GUS) reporter assay in pMTP1::*GUS* plants. pAtMTP1, *Arabidopsis thaliana MTP1* promoter; pAhMTP1, *Arabidopsis halleri MTP1* promoters. (a) Qualitative GUS reporter assay in pAtMTP1::*GUS* plants (upper pictures) and pAhMTP1-γ::*GUS* plants (lower pictures): (from left to right) 3-wk-old leaves, inflorescence, roots, stomata and trichomes. (b) Qualitative GUS reporter assay in 10-d-old plantlets: (from left to right) 35S CaMV::*GUS*, pAtMTP1::*GUS*, pAhMTP1-α::*GUS*, pAhMTP1-β::*GUS*, pAhMTP1-γ::*GUS*. (c) Quantitative GUS reporter assay. In (a) and (b), representative plants are shown for each construct, while (c) represents the results obtained considering three independent homozygous lines carrying single insertion of the indicated constructs. In (c), data are represented as means ± SD; lowercase letters indicate statistical significance, evaluated by Welch's ANOVA followed by a Games–Howell *post hoc* test ($P < 0.05$).

other *cis*-acting elements (Fig. 5a). *GUS* expression driven by the resulting mut303/400 promoter showed the same profile as the wild-type pAhMTP1-γ promoter, but was higher in both shoots and roots when measured by real-time RT-PCR (Fig. 5b,c), with a particularly marked difference in leaves, as indicated by arrows in Fig. 5(b).

Site-directed mutagenesis of MYB-binding sites

As shown in Fig. 2(a), pAhMTP1, but not pAtMTP1, drives *GUS* expression in leaf trichomes. MYB-binding sites have been proposed as correlated with trichome-specific expression (Wang *et al.*, 2002). To confirm the ability of these motifs to drive expression

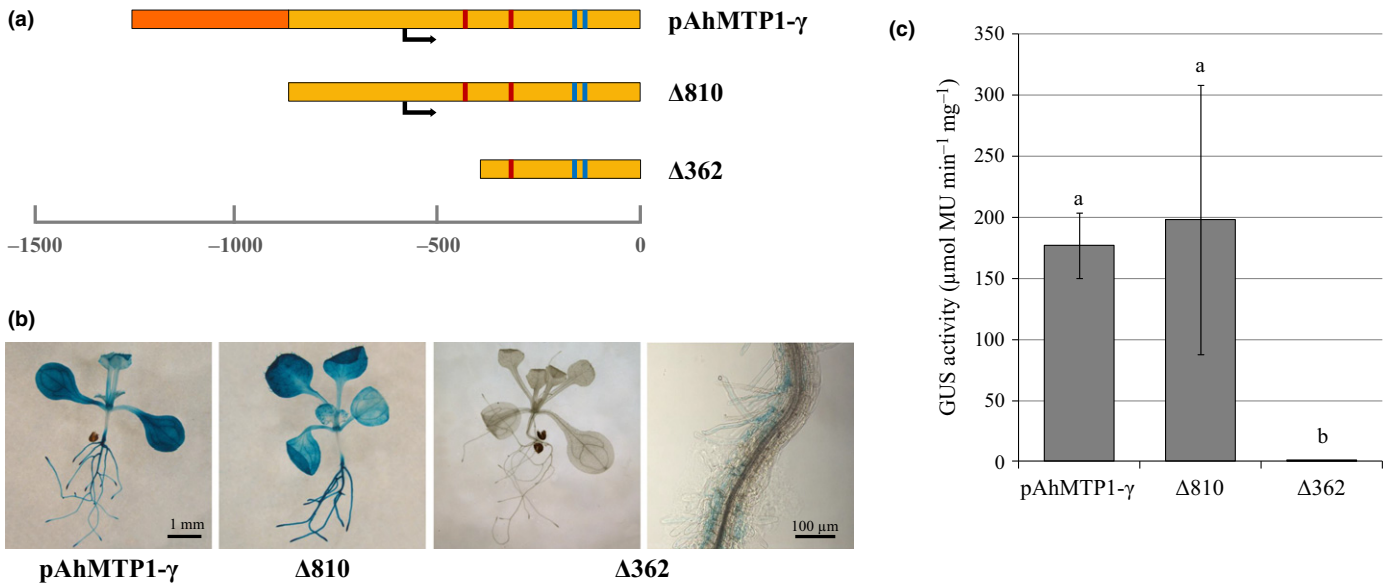

Fig. 3 β-Glucuronidase (GUS) reporter assay on the truncated forms of the *Arabidopsis halleri MTP1* promoter. pAhMTP1-γ, entire *A. halleri MTP1* promoter; Δ810, 810 bp-long truncated form; Δ362, 362 bp-long truncated form. (a) Schematic representation of the truncated forms of pAhMTP1-γ. (b) Qualitative GUS reporter assay in 10-d-old plantlets transformed with the entire and truncated *A. halleri MTP1* promoters: (from left to right) pAhMTP1-γ::*GUS*, Δ810::*GUS*, Δ362::*GUS*, detail of the roots of the Δ362::*GUS* plants. (c) Quantitative GUS reporter assay. In (a) and (b), representative plants are shown for each construct, while (c) represents the results obtained considering three independent homozygous lines carrying single insertion of the indicated constructs. In (c), data are represented as means ± SD; lowercase letters indicate statistical significance, evaluated by Welch's ANOVA followed by a Games–Howell *post hoc* test ($P < 0.05$).

```
pAtMTP1      -125 TGCTTTCTTTTTTGTTGAAACAGATCACCAAATA-AGAAAACTCTTGTGGTTCT--ATTG -182
pAlMTP1      -138 TGCTTTCTTTTTTATTGAAACAGATTGCCAAATTCAGAAAACTGTTGTGCTTCT--ATTG -196
pAhMTP1_α    -113 TGCTTTCTTTTCTGTTGAAACAGTTTACCAAGTTCAGAAAACTGTTGTGCTTCT--ATTG -171
pAhMTP1_β    -113 TGCTTTCTTTTCTGTTGAAACAGTTTACCAAGTTCAGAAAACTGTTGTGCTTCT--ATTG -171
pAhMTP1_γ    -113 TGCTTTCTTTTCTGTTGAAACAGTTTACCAAGTTCAGAAAACTGTTGTGCTTCT--ATTG -171
pAhMTP1_A1    -96 TGCTTTCTTTTCTGTTGAAACAGTTTACCAAGTTCAGAAAACTGTTGTGCTTCT--ATTG -154
pAhMTP1_A2    -96 TGCTTTCTTTTCTGTTGAAACAGTTTACCAAGTTCAGAAAACTGTTGTGCTTCT--ATTG -154
pAhMTP1_B    -112 TGCTTTCTTTTCTGTTGAAACAGTTTACCAAGTTCAGAAAACTGTTGTGCTTCTCTATTG -172
pAhMTP1_C    -112 TGCTTTCTTTTCTGTTGAAACAGTTTACCAAGTTCAGAAAACTGTTGTGCTTCT--ATTG -170
pAhMTP1_D    -113 TGCTTTCTTTTCTGTTGAAACAGTTTACCAAGTTCAGAAAACTGTTGTGCTTCT--ATTG -171
                  ********** * ******** *  **** *  ******** ***** ****  ****
```

Fig. 4 Alignment of the *MTP1* promoters of *Arabidopsis thaliana*, *Arabidopsis lyrata* and *Arabidopsis halleri* in the region of the tandem MYB-binding sites (in green letters). The equivalent *A. thaliana* and *A. lyrata* sites are indicated in red letters. pAtMTP1, *A. thaliana MTP1* promoter; pAlMTP1, *A. lyrata MTP1* promoter; pAhMTP1, *A. halleri MTP1* promoters. Asterisks under the alignment indicate nucleotide conservation in all the sequences considered.

in trichomes, site-directed mutagenesis was used to introduce single-base mutations in one or both MYB-binding motifs in the pAhMTP1-γ promoter (mut155 and mut125/155). These mutations reproduce the *A. thaliana* sequence (Fig. 6a). *GUS* expression in plants transformed with the mut155::*GUS* and mut125/155::*GUS* constructs was absent in the trichomes of fully expanded leaves, confirming that these MYB-binding sites are required for *MTP1* expression in *A. halleri* trichomes (Figs 6b, S3).

Involvement of MYB-binding motifs in Zn tolerance and accumulation

The necessity of MYB-binding sites for the specific expression of *MTP1* in *A. halleri* trichomes prompted us to investigate their involvement in Zn tolerance. *A. thaliana mtp1* mutant plants transformed with the constructs pAhMTP1-γ::*AtMTP1* and mut125/155::*AtMTP1* were tested *in vitro* in the presence of 300 and 500 μM $ZnSO_4$ (Fig. 7a). In terms of root length (Fig. 7b), biomass (Fig. 7c) and Chl content (Fig. 7d), transformation with pAhMTP1-γ::*AtMTP1* was able to restore Zn tolerance in the *mtp1* background. On the other hand, *mtp1* plants harboring the mut125/155::*AtMTP1* construct were significantly more sensitive to Zn excess, similar to what was observed for *mtp1* mutants.

Since *MTP1* overexpression induces a different Zn distribution in *A. thaliana* (van der Zaal *et al.*, 1999), Zn accumulation was also investigated in control plants and *mtp1* transformed with the pAhMTP1::*AtMTP1* and mut125/155::*AtMTP1* vectors after exposure to 0.7 μM $ZnSO_4$ (standard conditions) and

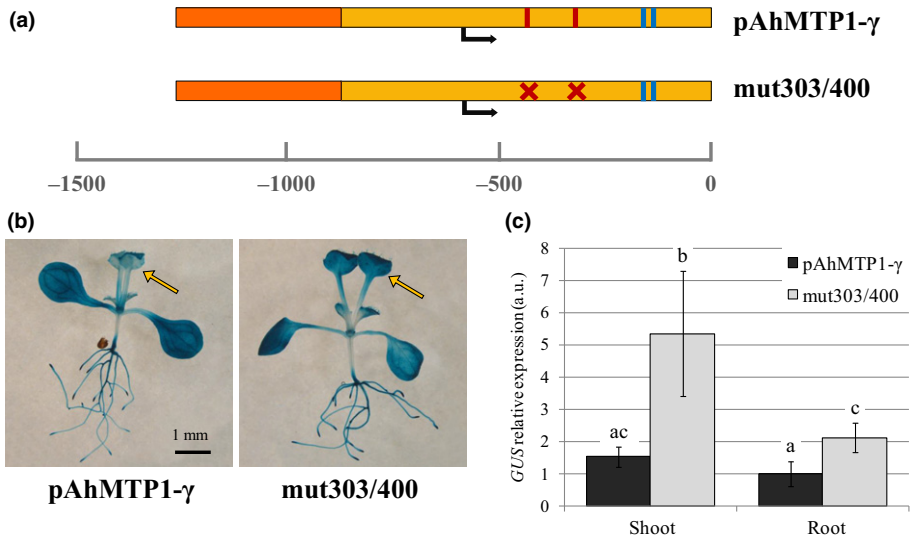

Fig. 5 β-Glucuronidase (GUS) reporter assay on the mutated form of the *Arabidopsis halleri MTP1* promoter lacking the two *telo*-box motifs (mut303/400). pAhMTP1-γ, wild-type *A. halleri MTP1* promoter. (a) Schematic representation of the mutated promoter: *telo*-boxes are indicated by red bars, mutated sites by red crosses. (b) Qualitative GUS reporter assay on 10-d-old plantlets transformed with the pAhMTP1-γ promoter (left) and the mut303/400 promoter (right); arrows highlight the different staining intensity in leaves. (c) Quantitative GUS assay by real-time reverse transcription polymerase chain reaction. In (b), representative plants are shown for each construct, while (c) represents the results obtained considering three independent homozygous lines carrying single insertion of the indicated constructs. In (c), data are represented as means ± SD; lowercase letters indicate statistical significance, evaluated by Welch's ANOVA followed by a Games–Howell *post hoc* test ($P < 0.05$).

25 μM $ZnSO_4$ (excess Zn conditions). Under Zn excess, the leaves of the mut125/155*::AtMTP1* transgenic plants accumulated more Zn (Fig. 8a), whereas in roots, Zn concentrations were *c.* 50% higher in pAhMTP1-γ*::AtMTP1* plants than in all other genotypes (Fig. 8b). Significant differences were also observed in roots under control conditions, with mut125/155*::AtMTP1* plants accumulating lower metal concentrations (Fig. 8b).

Zn accumulation in trichomes was analyzed by ESEM-EDS in plants grown in 0.7 μM (standard conditions) and 25 μM $ZnSO_4$. Zn was not detected along the entire body of the trichome but only in a ring at the trichome base (Fig. 9a), as previously reported for *A. halleri* (Zhao *et al.*, 2000; Sarret *et al.*, 2009) and *A. thaliana* (Ager *et al.*, 2003; Isaure *et al.*, 2006). Zn accumulating in this region was therefore used for a semiquantitative comparison among the lines. Zn was not detectable in the trichomes of plants grown under standard conditions; in the presence of 25 μM $ZnSO_4$, the Zn content of the trichomes of mut125/155*::AtMTP1* plants was significantly lower than that of both control and pAhMTP1*::AtMTP1* plants (Fig. 9b).

Comparison of *MTP1* promoter sequences in the Brassicaceae family

To investigate the role of *cis*-regulation in the *MTP1* promoter in more detail, a variety of Brassicaceae species were compared, including both metallophyte (*A. halleri* I16, *C. resedifolia*, *N. caerulescens*, *N. praecox*) and nonmetallophyte species (*A. thaliana*, *A. lyrata*, *C. officinalis*, *S. officinale*, *D. sophia*, *T. arvense*). *MTP1* promoter sequences were obtained by genome walking, with the exception of the *A. thaliana* and *A. lyrata* sequences, which were retrieved from TAIR. The sequences ranged in length from *c.* 600 bp (*C. officinalis*) to *c.* 2000 bp (*C. resedifolia*). The first 600 bp of each sequence were only moderately conserved, with a mean pairwise identity of 37%. Multiple Em for Motif Elicitation (MEME) analysis to identify conserved motifs among the different Brassicaceae *MTP1* promoters (Fig. S4; Table S4) revealed no statistically significant association between motif occurrence and the metallophyte status of the species considered, indicating that the identified motifs are probably not involved in the evolution of heavy metal hypertolerance. The most significant conserved motif was the *telo*-box (Table S4), whose involvement in *MTP1* regulation has been investigated in this work.

Discussion

Although copy number expansion and transcriptional up-regulation have been proposed to contribute to the higher expression levels observed for hypertolerance/hyperaccumulation determinants, as *MTP1* in hyperaccumulator species (Shahzad *et al.*, 2010), there is no characterization of the differential regulation of *MTP1* in metallophyte hyperaccumulators and nonmetallophyte species. We chose to perform our study on the metallicolous *A. halleri* I16, which is characterized by both hypertolerance and hyperaccumulation of Zn. Similarly to *A. halleri* Auby, this population grows in soils highly contaminated with Zn, Cd and lead (Pb) (Meyer *et al.*, 2015) and displays very high Zn accumulation levels (Decombeix, 2011).

The three novel *MTP1* promoter sequences amplified from *A. halleri* I16 share high sequence identity in the first 800 bp upstream of the start codon with the five promoters found in the Auby ecotype (Shahzad *et al.*, 2010). Remarkable sequence conservation was observed in the 5′UTR compared with the

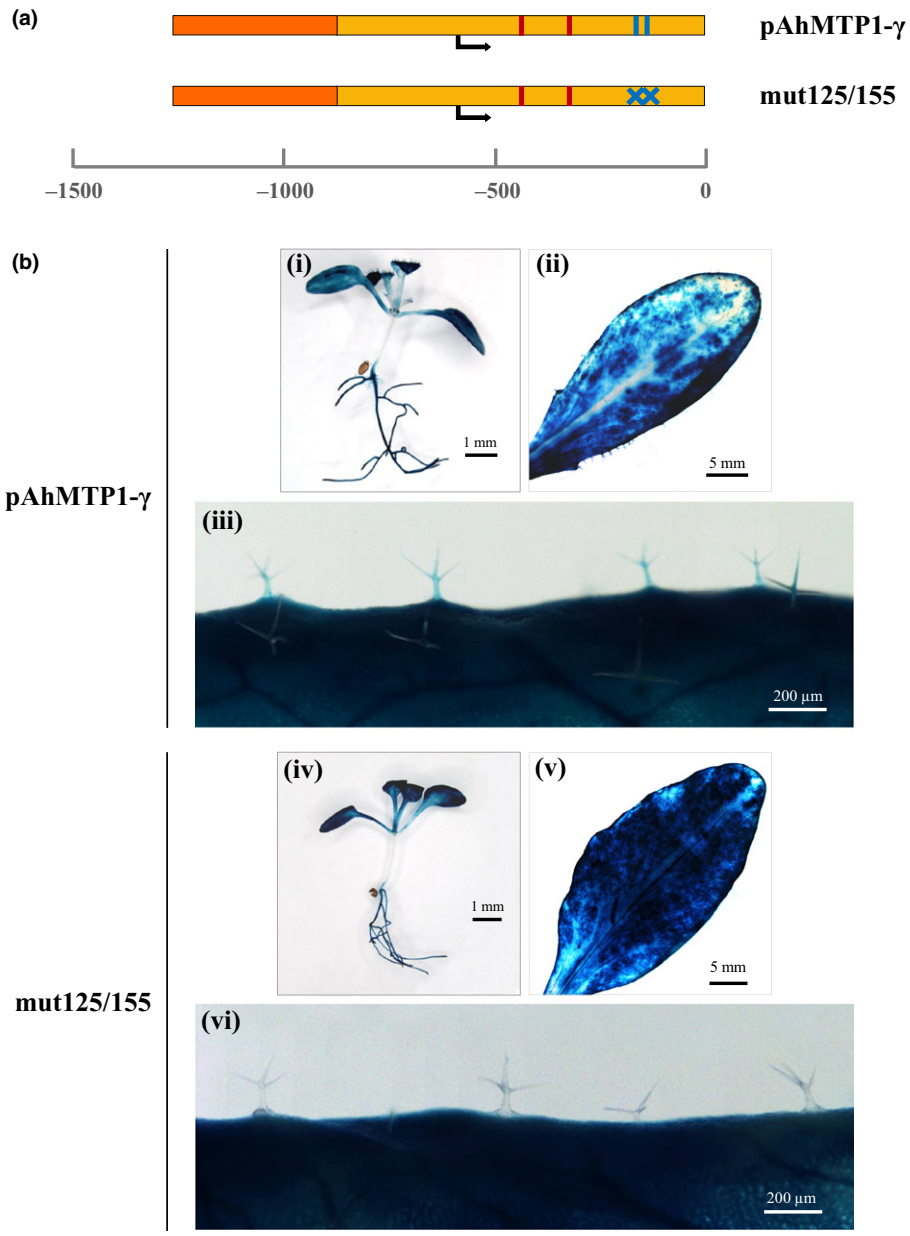

Fig. 6 β-Glucuronidase (GUS) reporter assay on the mutated form of the *Arabidopsis halleri MTP1* promoter lacking the two MYB-binding sites (mut125/155). pAhMTP1-γ, wild-type *A. halleri MTP1* promoter. (a) Schematic representation of the mutated promoter: MYB-binding sites are indicated by blue bars, mutated sites by blue crosses. (b) Qualitative reporter GUS assay on the wild-type pAhMTP1-γ promoter and the mut125/155 promoter showing: (i, iv) 10-d-old plantlets; (ii, v) leaves of 3-wk-old plants; and (iii, vi) trichomes on 3-wk-old leaves. Representative plants are shown for each construct.

corresponding *A. thaliana* and *A. lyrata* sequences, as reported previously for the Auby population (Shahzad *et al.*, 2010). The tentative amplification of ecotype I16 promoter sequences equivalent to *AhMTP1-A1/A2/B/C/D* in the *A. halleri* Auby population, performed with discriminating primers designed upstream the 800-bp-long conserved region of the promoters, provided positive results only for the D copy. It is therefore plausible that the geographically distant populations I16 and Auby, belonging to different phylogeographic units that have evolved independently since the Last Glacial Maximum (Pauwels *et al.*, 2012), have diverged in the distal region of the *MTP1* promoters. The novel promoters identified herein have acquired different transcription abundances. Owing to the lack of genomic information data and the limit imposed by the genome walking technique, the genomic context of each copy remains unknown, and therefore it cannot be determined whether the four sequences identified are allelic variants or distinct *loci*.

As *AhMTP1-D* has been discussed in previous reports (Shahzad *et al.*, 2010), we focused on the three novel *MTP1* promoters. All four *AhMTP1* sequences identified were actively transcribed in *A. halleri* I16, as highlighted by real-time RT-PCR. By quantitative GUS assay, the *A. halleri MTP1*-α/β/γ promoters were more active than the *A. thaliana MTP1* promoter, suggesting that the higher *MTP1* expression levels in *A. halleri* reflect a combination of copy number expansion and transcriptional regulation. The 800 bp proximal region, including the 5′UTR of the *MTP1* mRNA, was highly conserved among all *AhMTP1* promoter sequences, and is thus probably the functional core of the *A. halleri MTP1* promoter, as confirmed by the comparable expression levels conferred by the *AhMTP1*-γ promoter and the

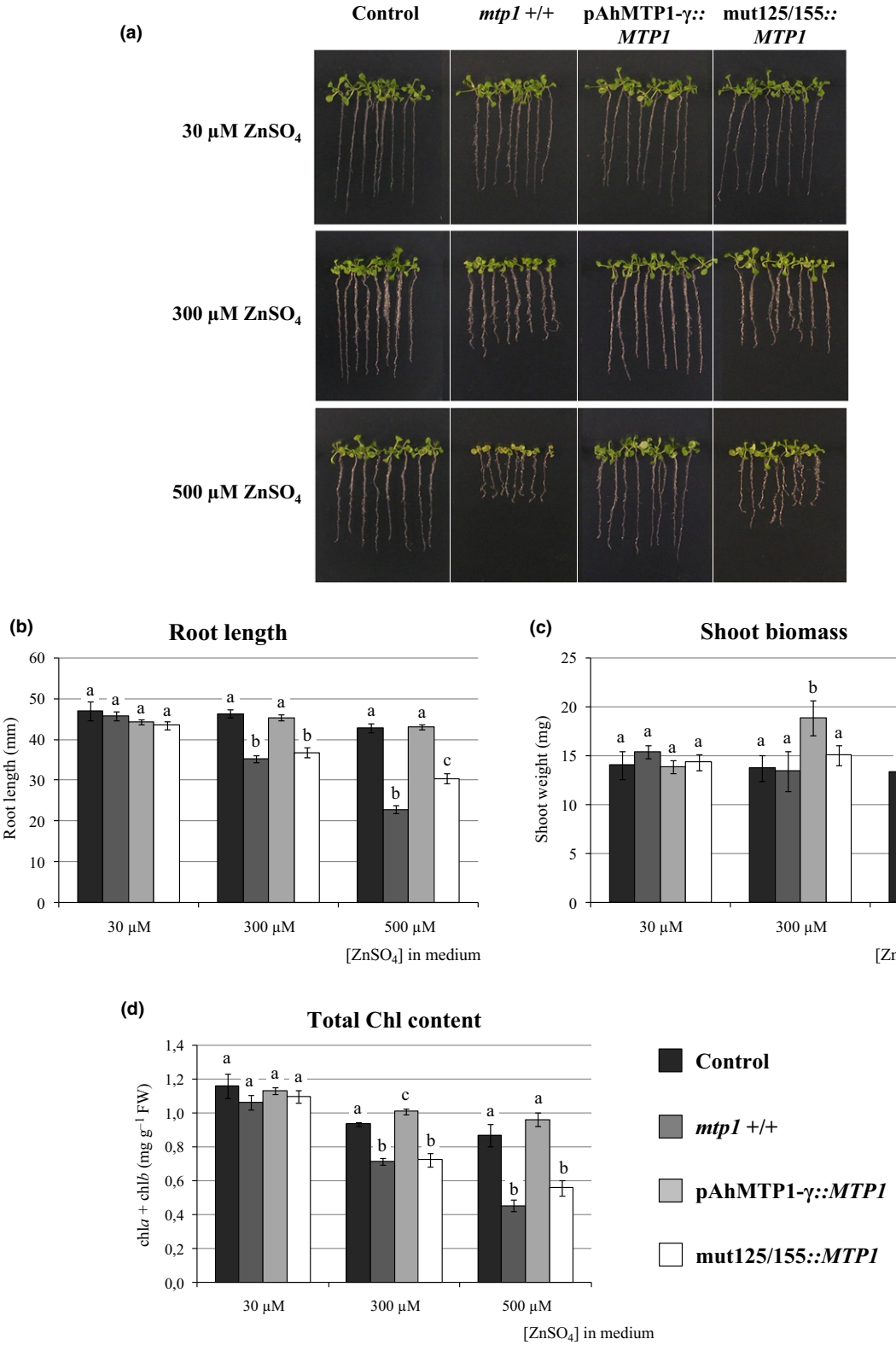

Fig. 7 Analysis of zinc (Zn) tolerance in control (empty vector), *mtp1* mutant, and *mtp1* pAhMTP1-γ::*AtMTP1* and mut125/155::*AtMTP1* plantlets grown in standard MS medium (30 µM $ZnSO_4$) and excess Zn (300 and 500 µM $ZnSO_4$). (a) Genotypes after the different Zn treatments. (b) Root length; (c) shoot biomass; (d) total Chl content. pAhMTP1-γ, wild-type *Arabidopsis halleri MTP1* promoter; mut125/155, *A. halleri MTP1* promoter lacking the two MYB-binding sites. Statistical comparisons refer to the different genotypes under the same Zn condition. Data are represented as means ± SD; lowercase letters indicate statistical significance, evaluated by Welch's ANOVA followed by a Games–Howell *post hoc* test ($P < 0.05$).

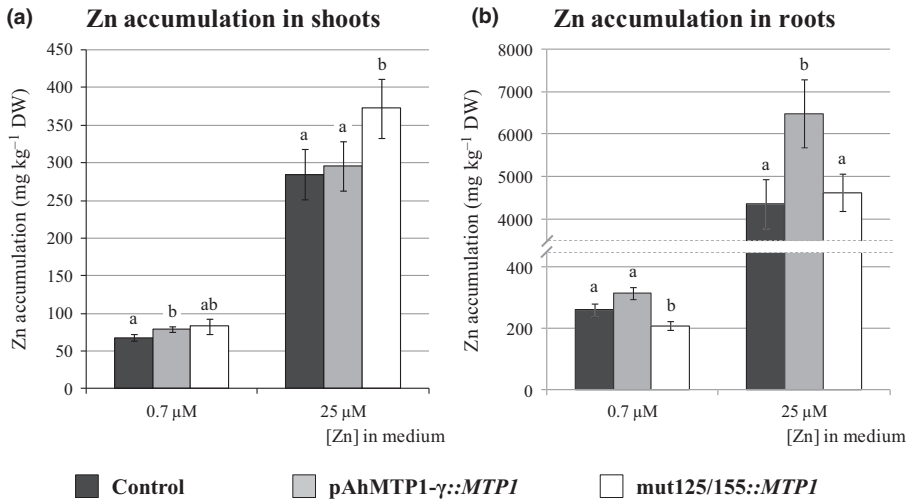

Fig. 8 Analysis of zinc (Zn) accumulation in the shoots (a) and roots (b) of control (empty vector) plants and *mtp1* transformed with pAhMTP1-γ::*AtMTP1* and mut125/155::*AtMTP1* constructs. The plants were grown in standard Hoagland's solution (0.7 µM $ZnSO_4$) and in excess Zn (25 µM $ZnSO_4$). pAhMTP1-γ, wild-type *Arabidopsis halleri MTP1* promoter; mut125/155, *A. halleri MTP1* promoter lacking the two MYB-binding sites. Statistical comparisons refer to the different genotypes under the same Zn condition. Data are represented as means ± SD; lowercase letters indicate statistical significance, evaluated by Welch's ANOVA followed by a Games–Howell *post hoc* test ($P < 0.05$).

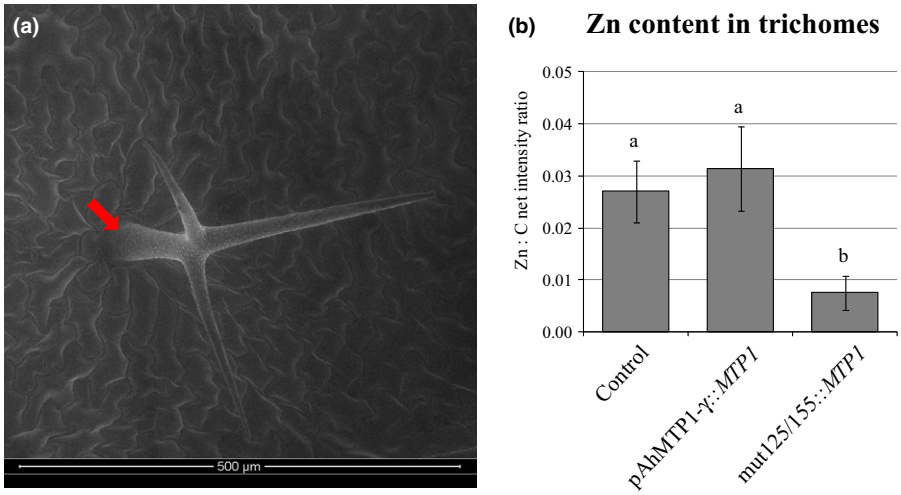

Fig. 9 Environmental scanning electron microscopy coupled with energy-dispersive X-ray spectroscopy (ESEM-EDS) analysis of zinc (Zn) accumulation in the trichomes of controls (empty vector transformed plants), *mtp1* plants transformed with pAhMTP1-γ::*AtMTP1*, and mut125/155::*AtMTP1* constructs grown under excess Zn conditions (25 µM $ZnSO_4$). pAhMTP1-γ, wild-type *Arabidopsis halleri MTP1* promoter; mut125/155, *A. halleri MTP1* promoter lacking the two MYB-binding sites. (a) ESEM micrograph: the trichome region used for spectral collection is indicated by the red arrow. (b) Mean Zn accumulation in trichomes, expressed as Zn : carbon (C) net intensity ratio. Data are represented as means ± SD; lowercase letters indicate statistical significance, evaluated by Welch's ANOVA followed by a Games–Howell *post hoc* test ($P < 0.05$).

corresponding Δ810 truncated form. Essential regulatory elements are situated between 362 and 810 bp upstream of the start codon because the Δ362 truncated promoter showed only minimal activity. Indeed, the transcriptional start site is predicted to lie 546 bp upstream of the start codon in the pAhMTP1-γ sequence, as inferred by alignment with the *A. thaliana* promoter. The *A. thaliana*, *A. lyrata* and *A. halleri MTP1* promoters lack a TATA box, which is not unexpected because this element is only found in 25% of *A. thaliana* promoters (Yamamoto *et al.*, 2009). Interestingly, an initiator element previously identified in the TATA-less promoter of the light-induced tobacco gene *PsaDb* (Nakamura *et al.*, 2002) was found close to the transcriptional start site in all the promoters, suggesting that this element controls the transcriptional initiation of the *MTP1* gene.

The expression profile conferred by the *A. thaliana* and *A. halleri* I16 *MTP1* promoters showed marked differences as revealed by GUS reporter assays. The stronger expression driven by the three *AhMTP1* promoters is consistent with the key role of MTP1 in vacuolar Zn transport in the hyperaccumulator *A. halleri*. Whereas pAhMTP1 resulted in GUS staining in the whole plant, the activity of the *A. thaliana* promoter in the leaves was restricted to the vascular tissues, hydathodes and guard cells. The expression in the latter, common to both *A. thaliana* and *A. halleri*, is associated with the presence of clusters of

Dof-binding sites in the promoters (Plesch *et al.*, 2001; Galbiati *et al.*, 2008; Cominelli *et al.*, 2011). Indeed, the stomatal expression previously reported for the *A. thaliana MTP1* promoter (Kawachi *et al.*, 2009) has also been observed for other transporters involved in metal accumulation, such as *A. thaliana HMA3* (Morel *et al.*, 2009) and *MTP11* (Peiter *et al.*, 2007) and *N. caerulescens ZNT1* (Küpper *et al.*, 2007). As also proposed for *HMA3* (Morel *et al.*, 2009), *MTP1* expression in the guard cells of both nonaccumulator and hyperaccumulator species may be necessary to prevent metal toxicity and the subsequent impairment of stomatal functions. The prevalence of this motif in the promoters of nonmetallophyte species probably ensures the functionality of guard cells, whereas hyperaccumulators rely on the combined effect of diverse metal tolerance mechanisms, as also suggested by the low metal concentrations in the stomatal complexes of several hyperaccumulator species (Frey *et al.*, 2000; Psaras *et al.*, 2000; Küpper *et al.*, 2001). Several root-specific *cis*-acting elements were identified in all the *MTP1* promoters, but the *telo*-box is the most interesting, as it is conserved in *MTP1* promoters from several hyperaccumulator and nonaccumulator Brassicaceae species. The *telo*-box has been found in genes encoding components of the translational machinery and redox balance system (Regad *et al.*, 1995; Tremousaygue *et al.*, 1999; Gaspin *et al.*, 2010) and is necessary for gene expression in root primordia (Tremousaygue *et al.*, 1999; Manevski *et al.*, 2000). In the *A. thaliana*, *A. lyrata* and *A. halleri MTP1* promoters, the *telo*-box elements are located in the 5′UTR as previously reported for genes involved in translation (Tremousaygue *et al.*, 1999). Site-directed mutagenesis of these motifs in the *A. halleri* promoter (mut303/400) enhanced *GUS* expression in the shoots and roots without affecting the spatial expression pattern. Although this result contrasts with previous reports (Tremousaygue *et al.*, 1999; Manevski *et al.*, 2000), a similar phenotype was reported following the deletion of a *telo*-box in the *A. thaliana EF-1α* gene (Curie *et al.*, 1993). Furthermore, the consequences of site-directed mutagenesis in the *A. halleri* promoter are consistent with the presence of an additional *telo*-box motif in the *A. thaliana* and *A. lyrata* promoters, suggesting that this element may be involved in the negative regulation of the *MTP1* promoter. The lack of motifs generally associated with *telo*-boxes in the *A. thaliana*, *A. lyrata* and *A. halleri* promoter sequences indicates that other *cis*-acting elements probably cooperate with *telo*-boxes in the *MTP1* promoters to confer expression profiles other than the root meristem-specific pattern previously described.

In addition to *telo*-boxes, root-specific ATATT motifs possibly involved in root-specific expression in the vasculature (Elmayan & Tepfer, 1995) were found in the promoters of all species considered, and root hair-specific *cis*-acting elements (Kim *et al.*, 2006; Won *et al.*, 2009) were found in pAtMTP1 and pAhMTP1. As the Δ362 truncated *A. halleri* promoter induced weak *GUS* expression in roots, some other unknown root-specific elements must be present in the most proximal region of the promoter, as neither ATATT nor root hair-specific *cis*-acting elements are located in this portion of pAhMTP1.

In contrast to the *A. thaliana* sequence, the *A. halleri MTP1* promoters identified herein conferred strong expression in the leaf mesophyll and trichomes. High levels of MTP1 in mesophyll cells may account for the high Zn tolerance observed in *A. halleri* compared with *A. thaliana*. No *cis*-acting elements for the induction of mesophyll-specific expression were identified by *in silico* analysis, and although several light-response elements were found, these cannot be responsible for the higher expression level in *A. halleri* because they were also present in the *A. thaliana* promoter. Therefore, pAhMTP1-driven mesophyll expression is possibly a result of as yet unknown elements or of specific combinations of known motifs.

A pair of MYB-binding motifs was found to be highly conserved in all *A. halleri MTP1* promoters analyzed, but these are absent in the *A. thaliana* and *A. lyrata* promoters as a result of single nucleotide substitutions, despite the generally high conservation in this region. MYB-binding sites were found as involved in the expression regulation of some trichome-specific genes (Szymanski *et al.*, 1998; Wang *et al.*, 2004; Pesch & Hülskamp, 2011). In detail, the MYB-binding motif CTGTTG was proposed to drive trichome-specific expression in the tobacco *CYP71D16* promoter (Wang *et al.*, 2002) and is able to bind the TT2 (TRANSPARENT TESTA 2)/AtMYB123 transcription factor, one of the partners of the TTG1 (TRANSPARENT TESTA GLABRA 1) WD40-repeat protein, involved in seed coat pigmentation, trichome initiation and development (Thévenin *et al.*, 2012). Site-directed mutagenesis of one (mut155) or both CTGTTG motifs to mimic the *A. thaliana* promoter (mut125/155) abolished *GUS* expression in trichomes, thus confirming the role of these MYB-binding motifs in *MTP1* expression in trichomes. A search for the paired CTGTTG sequences in the 5′UTR of *A. thaliana* genes, whose orthologous are involved in metal tolerance and accumulation in the hyperaccumulator species *A. halleri* and *N. caerulescens*, revealed their absence. This result is consistent with a putative role of this motif in the evolution of the *A. halleri* hypertolerance phenotype. Such a hypothesis is also supported by Zn tolerance experiments, in which the mut125/155*::AtMTP1* transgenic plants were less tolerant than the plants transformed with the cassette containing the wild-type *A. halleri* promoter. MEME analysis of the *MTP1* promoter in different Brassicaceae species did not reveal any association between this motif and hypertolerant/hyperaccumulator species; indeed the paired MYB-binding sites were unique to the *A. halleri* promoter. The lack of this *cis*-acting element in the *MTP1* promoters of *Noccaea* species may correlate with the absence of trichomes on their leaves (Al-Shehbaz *et al.*, 2006). Genome walking along *MTP1* promoters from the Brassicaceae species considered did not identify any specific feature correlating with the hypertolerance/hyperaccumulation trait. By contrast, promoter sequence homology reflected the phylogenetic proximity of the species – regardless of their status as metallophyte or not – consistently with the hypothesis that hypertolerance/hyperaccumulation has evolved independently several times in the Brassicaceae lineage (Krämer *et al.*, 2007; Krämer, 2010). In this context, species derived from different evolutionary events are likely to have selected unrelated *cis*-acting modifications to increase *MTP1* expression levels as

well as different strategies to cope with excess metals, for example *MTP1* expression in trichomes in the case of *A. halleri*.

MTP1 expression in *A. halleri* trichomes is remarkable because metal accumulation in trichomes has been reported in many hyperaccumulator species, as *A. halleri* (Küpper *et al.*, 2000; Zhao *et al.*, 2000; Sarret *et al.*, 2002), *Alyssum murale* (Broadhurst *et al.*, 2004) and *Astragalus bisulcatus* (Freeman *et al.*, 2006). However, other hyperaccumulators rely on different cell types for metal storage (Cosio *et al.*, 2005; Freeman *et al.*, 2006). On the other hand, metal storage in trichomes is not exclusive to hyperaccumulators, given that this process also occurs in *A. thaliana* (Ager *et al.*, 2003; Isaure *et al.*, 2006) and *A. lyrata* (Sarret *et al.*, 2009). In *A. halleri*, trichomes can accumulate substantially higher concentrations of metal than surrounding cells, but they constitute only a minor portion of the whole leaf biomass and therefore cannot be considered a major metal storage site (Küpper *et al.*, 2000; Sarret *et al.*, 2002, 2009; Huguet *et al.*, 2012). Increasing metal concentrations (Küpper *et al.*, 2000) or longer metal exposure times (Huguet *et al.*, 2012) progressively saturate trichomes, whereas metal concentrations continue to increase in the mesophyll cells. These data support the hypothesis that trichomes are involved in short-term tolerance rather than long-term metal hyperaccumulation. Therefore, the role of *MTP1* expression in trichomes was investigated in more detail in *A. thaliana*.

The *mtp1* plants transformed with the pAhMTP1-γ*::AtMTP1* cassette tolerated excess Zn well and were mostly insensitive to the high metal concentrations under the conditions tested. By contrast, excess Zn had a significant impact on plant growth in the mut125/155*::AtMTP1* lines, showing hypersensitivity similar to the *mtp1* mutant. Overall, these results indicate a role of the MYB-binding motifs in metal tolerance in *A. thaliana*, supporting their involvement in the evolution of Zn hypertolerance in *A. halleri*.

Zinc accumulation was also considered in the *A. thaliana mtp1* transgenic lines containing the pAhMTP1-γ*::AtMTP1* and mut125/155*::AtMTP1* cassettes. When exposed to Zn excess, plants transformed with the mut125/155*::AtMTP1* construct accumulated lower concentrations of Zn in trichomes than did control and pAhMTP1-γ*::AtMTP1* transgenic lines, supporting the role of the MYB-binding motifs studied here in directing *MTP1* expression in trichomes. Moreover, in these growth conditions, pAhMTP1-γ*::AtMTP1* plants accumulated the highest concentrations of Zn in the roots, as observed previously for plants overexpressing *AtMTP1* (van der Zaal *et al.*, 1999); on the other hand, plants expressing mut125/155*::AtMTP1* accumulated more Zn in the shoot. This different distribution observed between the two transgenic genotypes was unexpected, as, by GUS assay, MYB-binding sites seemed linked only with expression in trichomes; however, the higher root Zn accumulation in the pAhMTP1-γ*::AtMTP1* lines suggests an increased Zn retention in roots owing to a possible control of these *cis* elements on *MTP1* expression in roots as well. In fact, an eventual difference in *GUS* expression in specific root tissues may be masked by the high global root staining observed in GUS assay. In fact, the different metal distribution probably explains the noteworthy phenotype observed in the tolerance analysis: metal compartmentalization in root cells is a common mechanism for metal tolerance, known as the excluder strategy (Baker, 1981; Krämer, 2010). Indeed, the model system *A. thaliana*, used as a background for transformation, lacks the up-regulation of other determinants for hypertolerance and hyperaccumulation, as HMA4 (Willems *et al.*, 2007; Frérot *et al.*, 2010; Meyer *et al.*, 2016), and relies on the excluder strategy to cope with metal stress (Becher *et al.*, 2004). In this view, the higher Zn translocation to shoots observed in mut125/155*::AtMTP1* plants combines with the reduced storage in the trichomes, resulting in the Zn-sensitive phenotype observed in this genotype. It is evident that Zn tolerance does not depend solely on Zn storage in the trichomes; however, the results of this study indicate that the role of this cell type in the evolution of hypertolerance is not negligible. Globally, these results underline the essential role of *MTP1* expression regulation in the response to excess Zn, supporting the importance of this vacuolar transporter in the evolution of the hypertolerance trait in metallicolous populations of *A. halleri* (Dräger *et al.*, 2004; Willems *et al.*, 2007; Meyer *et al.*, 2016).

In conclusion, the differential *cis*-regulation of *MTP1* expression in *A. thaliana* and *A. halleri*, combined with the *MTP1* copy number expansion in the latter, led to the overexpression of this transporter in *A. halleri*. Interestingly, among the *cis*-acting elements identified in the promoters we analyzed, the MYB-binding sites located in the 5′UTR of the *A. halleri MTP1* gene mark the divergent evolution between the hyperaccumulator species *A. halleri* and the nonaccumulators *A. thaliana* and *A. lyrata*. In addition, our data indicate that these motifs play a notable role in metal tolerance, demonstrating the importance of efficient expression regulation of genetic determinants for the evolution of a complex extremophile trait such as Zn hypertolerance.

Acknowledgements

We are grateful to Dr Mirca Lazzaretti (University of Parma) for her assistance with photography. Funding for E.F.'s PhD was from MIUR (the Italian Ministry of University and Research).

Author contributions

E.F. performed most of the experiments and wrote the article with contribution of A.F. and G.D. C.V. and M.L. amplified the Brassicaceae promoter sequences and helped with the bioinformatic analysis. G.V. and M.M. analyzed the zinc content in trichomes. A.F. and G.D. conceived the project and supervised the experiments.

References

Ager FJ, Ynsa MD, Domínguez-Solís JR, López-Martín MC, Gotor C, Romero LC. 2003. Nuclear micro-probe analysis of *Arabidopsis thaliana* leaves. *Nuclear Instruments and Methods in Physics Research B* **210**: 401–406.

Al-Shehbaz IA, Beilstein MA, Kellogg EA. 2006. Systematics and phylogeny of the Brassicaceae (Cruciferae): an overview. *Plant Systematics and Evolution* **259**: 89–120.

Assunção AGL, Da Costa Martins P, De Folter S, Vooijs R, Schat H, Aarts MGM. 2001. Elevated expression of metal transporter genes in three accessions of the metal hyperaccumulator *Thlaspi caerulescens*. *Plant, Cell & Environment* **24**: 217–226.

Baker AJM. 1981. Accumulators and excluders – strategies in the response of plants to heavy metals. *Journal of Plant Nutrition* **3**: 643–654.

Baker AJM. 2002. In search of the Holy Grail – a further step in understanding metal hyperaccumulation? *New Phytologist* **155**: 1–7.

Becher M, Talke IN, Krall L, Krämer U. 2004. Cross-species microarray transcript profiling reveals high constitutive expression of metal homeostasis genes in shoots of the zinc hyperaccumulator *Arabidopsis halleri*. *Plant Journal* **37**: 251–268.

Bert V, Meerts P, Saumitou-Laprade P, Salis P, Gruber W, Verbruggen N. 2003. Genetic basis of Cd tolerance and hyperaccumulation in *Arabidopsis halleri*. *Plant and Soil* **249**: 9–18.

Bloß T, Clemens S, Nies DH. 2002. Characterization of the ZAT1p zinc transporter from *Arabidopsis thaliana* in microbial model organisms and reconstituted proteoliposomes. *Planta* **214**: 783–791.

Broadhurst CL, Chaney RL, Angle JS, Maugel TK, Erbe EF, Murphy CA. 2004. Simultaneous hyperaccumulation of nickel, manganese, and calcium in *Alyssum* leaf trichomes. *Environmental Science and Technology* **38**: 5797–5802.

Cervera M. 2004. Histochemical and fluorometric assays for uidA (GUS) gene detection. In: Peña L, ed. *Transgenic plants: methods and protocols*. Totowa, NJ, USA: Humana Press, 203–214.

Cominelli E, Galbiati M, Albertini A, Fornara F, Conti L, Coupland G, Tonelli C. 2011. DOF-binding sites additively contribute to guard cell-specificity of *AtMYB60* promoter. *BMC Plant Biology* **11**: 162.

Cosio C, DeSantis L, Frey B, Diallo S, Keller C. 2005. Distribution of cadmium in leaves of *Thlaspi caerulescens*. *Journal of Experimental Botany* **56**: 765–775.

Courbot M, Willems G, Motte P, Arvidsson S, Roosens N, Saumitou-Laprade P, Verbruggen N. 2007. A major quantitative trait locus for cadmium tolerance in *Arabidopsis halleri* colocalizes with *HMA4*, a gene encoding a heavy metal ATPase. *Plant Physiology* **144**: 1052–1065.

Curie C, Axelos M, Bardet C, Atanassova R, Chaubet N, Lescure B. 1993. Modular organization and developmental activity of an *Arabidopsis thaliana EF-1α* gene promoter. *Molecular and General Genetics* **238**: 428–436.

Das M, Harvey I, Chu LL, Sinha M, Pelletier J. 2001. Full-length cDNAs: more than just reaching the ends. *Physiological Genomics* **6**: 57–80.

Decombeix I. 2011. *Etude de l'adaptation aux milieux calaminaires chez* Arabidopsis halleri*: approche écologique, génétique et phénotypique*. PhD thesis, École doctorale Sciences de la matière, du rayonnement et de l'environnement, Université des Sciences et Technologies de Lille 1, Lille, France. [WWW document] URL http://ori.univ-lille1.fr/notice/view/univ-lille1-ori-29234.

Desbrosses-Fonrouge AG, Voigt K, Schröder A, Arrivault S, Thomine S, Krämer U. 2005. *Arabidopsis thaliana* MTP1 is a Zn transporter in the vacuolar membrane which mediates Zn detoxification and drives leaf Zn accumulation. *FEBS Letters* **579**: 4165–4174.

Dräger DB, Desbrosses-Fonrouge AG, Krach C, Chardonnens AN, Meyer RC, Saumitou-Laprade P, Krämer U. 2004. Two genes encoding *Arabidopsis halleri MTP1* metal transport proteins co-segregate with zinc tolerance and account for high *MTP1* transcript levels. *Plant Journal* **39**: 425–439.

Elbaz B, Shoshani-Knaani N, David-Assael O, Mizrachy-Dagri T, Mizrahi K, Saul H, Brook E, Berezin I, Shaul O. 2006. High expression in leaves of the zinc hyperaccumulator *Arabidopsis halleri* of *AhMHX*, a homolog of an *Arabidopsis thaliana* vacuolar metal/proton exchanger. *Plant, Cell & Environment* **29**: 1179–1190.

Elmayan T, Tepfer M. 1995. Evaluation in tobacco of the organ specificity and strength of the *rolD* promoter, domain A of the 35S promoter and the 35S2 promoter. *Transgenic Research* **4**: 388–396.

Freeman JL, Zhang LH, Marcus MA, Fakra S, McGrath SP, Pilon-Smits EAH. 2006. Spatial imaging, speciation, and quantification of selenium in the hyperaccumulator plants *Astragalus bisulcatus* and *Stanleya pinnata*. *Plant Physiology* **142**: 124–134.

Frérot H, Faucon MP, Willems G, Godé C, Courseaux A, Darracq A, Verbruggen N, Saumitou-Laprade P. 2010. Genetic architecture of zinc hyperaccumulation in *Arabidopsis halleri*: the essential role of QTL × environment interactions. *New Phytologist* **187**: 355–367.

Frey B, Keller C, Zierold K, Schulin R. 2000. Distribution of Zn in functionally different leaf epidermal cells of the hyperaccumulator *Thlaspi caerulescens*. *Plant, Cell & Environment* **23**: 675–687.

Galbiati M, Simoni L, Pavesi G, Cominelli E, Francia P, Vavasseur A, Nelson T, Bevan M, Tonelli C. 2008. Gene trap lines identify *Arabidopsis* genes expressed in stomatal guard cells. *Plant Journal* **53**: 750–762.

Gaspin C, Rami JF, Lescure B. 2010. Distribution of short interstitial telomere motifs in two plant genomes: putative origin and function. *BMC Plant Biology* **10**: 283.

Guffanti AA, Wei Y, Rood SV, Krulwich TA. 2002. An antiport mechanism for a member of the cation diffusion facilitator family: divalent cations efflux in exchange for K^+ and H^+. *Molecular Microbiology* **45**: 145–153.

Hammond JP, Bowen HC, White PJ, Mills V, Pyke KA, Baker AJM, Whiting SN, May ST, Broadley MR. 2006. A comparison of the *Thlaspi caerulescens* and *Thlaspi arvense* shoot transcriptomes. *New Phytologist* **170**: 239–260.

Hanikenne M, Talke IN, Haydon MJ, Lanz C, Nolte A, Motte P, Kroymann J, Weigel D, Krämer U. 2008. Evolution of metal hyperaccumulation required *cis*-regulatory changes and triplication of *HMA4*. *Nature* **453**: 391–395.

Hoagland DR, Arnon DI. 1950. *The water-culture method for growing plants without soil. Circular 347*. Berkeley, CA, USA: College of Agriculture, University of California.

Huguet S, Bert V, Laboudigue A, Barthès V, Isaure MP, Llorens I, Schat H, Sarret G. 2012. Cd speciation and localization in the hyperaccumulator *Arabidopsis halleri*. *Environmental and Experimental Botany* **82**: 54–65.

Isaure MP, Fayard B, Sarret G, Pairis S, Bourguignon J. 2006. Localization and chemical forms of cadmium in plant samples by combining analytical electron microscopy and X-ray spectromicroscopy. *Spectrochimica Acta Part B: Atomic Spectroscopy* **61**: 1242–1252.

Kawachi M, Kobae Y, Mori H, Tomioka R, Lee Y, Maeshima M. 2009. A mutant strain *Arabidopsis thaliana* that lacks vacuolar membrane zinc transporter MTP1 revealed the latent tolerance to excessive zinc. *Plant and Cell Physiology* **50**: 1156–1170.

Kim DW, Lee SH, Choi SB, Won SK, Heo YK, Cho M, Park YI, Cho HT. 2006. Functional conservation of a root hair cell-specific *cis*-element in angiosperms with different root hair distribution patterns. *Plant Cell* **18**: 2958–2970.

Krämer U. 2010. Metal hyperaccumulation in plants. *Annual Review of Plant Biology* **61**: 517–534.

Krämer U, Talke IN, Hanikenne M. 2007. Transition metal transport. *FEBS Letters* **581**: 2263–2272.

Küpper H, Lombi E, Zhao FJ, McGrath SP. 2000. Cellular compartmentation of cadmium and zinc in relation to other elements in the hyperaccumulator *Arabidopsis halleri*. *Planta* **212**: 75–84.

Küpper H, Lombi E, Zhao FJ, Wieshammer G, McGrath SP. 2001. Cellular compartmentation of nickel in the hyperaccumulators *Alyssum lesbiacum*, *Alyssum bertolonii* and *Thlaspi goesingense*. *Journal of Experimental Botany* **52**: 2291–2300.

Küpper H, Seib LO, Sivaguru M, Hoekenga OA, Kochian LV. 2007. A method for cellular localization of gene expression via quantitative *in situ* hybridization in plants. *Plant Journal* **50**: 159–175.

Lamesch P, Berardini TZ, Li D, Swarbreck D, Wilks C, Sasidharan R, Muller R, Dreher K, Alexander DL, Garcia-Hernandez M *et al.* 2012. The Arabidopsis Information Resource (TAIR): improved gene annotation and new tools. *Nucleic Acids Research* **40**: D1202–D1210.

Livak KJ, Schmittgen TD. 2001. Analysis of relative gene expression data using real time quantitative PCR and the $2^{-\Delta\Delta CT}$ method. *Methods* **25**: 402–408.

Lombi E, Tearall KL, Howarth JR, Zhao FJ, Hawkesford MJ, McGrath SP. 2002. Influence of iron status on cadmium and zinc uptake by different ecotypes of the hyperaccumulator *Thlaspi caerulescens*. *Plant Physiology* **128**: 1359–1367.

Macnair MR, Bert V, Huitson SB, Saumitou-Laprade P, Petit D. 1999. Zinc tolerance and hyperaccumulation are genetically independent characters. *Proceedings of the Royal Society of London. Series B: Biological Sciences* **266**: 2175–2179.

Manevski A, Bertoni G, Bardet C, Tremousaygue D, Lescure B. 2000. In synergy with various *cis*-acting elements, plant insterstitial telomere motifs

regulate gene expression in Arabidopsis root meristems. *FEBS Letters* **483**: 43–46.

McDonald JH. 2014. *Handbook of biological statistics*, 3rd edn. Baltimore, MD, USA: Sparky House Publishing.

Meyer CL, Juraniec M, Huguet S, Chaves-Rodriguez E, Salis P, Isaure MP, Goormaghtigh E, Verbruggen N. 2015. Intraspecific variability of cadmium tolerance and accumulation, and cadmium-induced cell wall modifications in the metal hyperaccumulator *Arabidopsis halleri*. *Journal of Experimental Botany* **66**: 3215–3227.

Meyer CL, Pauwels M, Briset L, Godé C, Salis P, Bourceaux A, Souleman D, Frérot H, Verbruggen N. 2016. Potential preadaptation to anthropogenic pollution: evidence from a common quantitative trait locus for zinc and cadmium tolerance in metallicolous and nonmetallicolous accessions of *Arabidopsis halleri*. *New Phytologist* **212**: 934–943.

Morel M, Crouzet J, Gravot A, Auroy P, Leonhardt N, Vavasseur A, Richaud P. 2009. AtHMA3, a P1B-ATPase allowing Cd/Zn/Co/Pb vacuolar storage in Arabidopsis. *Plant Physiology* **149**: 894–904.

van de Mortel JE, Almar Villanueva L, Schat H, Kwekkeboom J, Coughlan S, Moerland PD, Loren Ver, van Themaat E, Koornneef M, Aarts MGM. 2006. Large expression differences in genes for iron and zinc homeostasis, stress response, and lignin biosynthesis distinguish roots of *Arabidopsis thaliana* and the related metal hyperaccumulator *Thlaspi caerulescens*. *Plant Physiology* **142**: 1127–1147.

Murashige T, Skoog F. 1962. A revised medium for rapid growth and bio assays with tobacco tissue cultures. *Physiologia Plantarum* **15**: 473–497.

Nakamura M, Tsunoda T, Obokata J. 2002. Photosynthesis nuclear genes generally lack TATA-boxes: a tobacco photosystem I gene responds to light through an initiator. *Plant Journal* **29**: 1–10.

Nies DH, Silver S. 1995. Ion efflux systems involved in bacterial metal resistances. *Journal of Industrial Microbiology* **14**: 186–199.

Nouet C, Charlier JB, Carnol M, Bosman B, Farnir F, Motte P, Hanikenne M. 2015. Functional analysis of the three *HMA4* copies of the metal hyperaccumulator *Arabidopsis halleri*. *Journal of Experimental Botany* **66**: 5783–5795.

Pauwels M, Vekemans X, Godé C, Frérot H, Castric V, Saumitou-Laprade P. 2012. Nuclear and chloroplast DNA phylogeography reveals vicariance among European populations of the model species for the study of metal tolerance, *Arabidopsis halleri* (Brassicaceae). *New Phytologist* **193**: 916–928.

Peiter E, Montanini B, Gobert A, Pedas P, Husted S, Maathuis FJM, Blaudez D, Chalot M, Sanders D. 2007. A secretory pathway-localized cation diffusion facilitator confers plant manganese tolerance. *Proceedings of the National Academy of Sciences, USA* **104**: 8532–8537.

Persans MW, Nieman K, Salt DE. 2001. Functional activity and role of cation-efflux family members in Ni hyperaccumulation in *Thlaspi goesingense*. *Proceedings of the National Academy of Sciences, USA* **98**: 9995–10000.

Pesch M, Hülskamp M. 2011. Role of *TRIPTYCHON* in trichome patterning in *Arabidopsis*. *BMC Plant Biology* **11**: 130.

Plesch G, Ehrhardt T, Mueller-Roeber B. 2001. Involvement of TAAAG elements suggests a role for Dof transcription factors in guard cell-specific gene expression. *Plant Journal* **28**: 455–464.

Porra RJ, Thompson WA, Kriedemann PE. 1989. Determination of accurate extinction coefficients and simultaneous equations for assaying chlorophylls *a* and *b* extracted with four different solvents: verification of the concentration of chlorophyll standards by atomic absorption spectroscopy. *Biochimica et Biophysica Acta - Bioenergetics* **975**: 384–394.

Psaras GK, Constantinidis T, Cotsopoulos B, Manetas Y. 2000. Relative abundance of nickel in the leaf epidermis of eight hyperaccumulators: evidence that the metal is excluded from both guard cells and trichomes. *Annals of Botany* **86**: 73–78.

Ramakers C, Ruijter JM, Lekanne Deprez RH, Moorman AFM. 2003. Assumption-free analysis of quantitative real-time polymerase chain reaction (PCR) data. *Neuroscience Letters* **339**: 62–66.

Regad F, Hervé C, Marinx O, Bergounioux C, Tremousaygue D, Lescure B. 1995. The *tef1* box, a ubiquitous *cis*-acting element involved in the activation of plant genes that are highly expressed in cycling cells. *Molecular and General Genetics* **248**: 703–711.

Sarret G, Saumitou-Laprade P, Bert V, Proux O, Hazemann JL, Traverse A, Marcus MA, Manceau A. 2002. Forms of zinc accumulated in the hyperaccumulator *Arabidopsis halleri*. *Plant Physiology* **130**: 1815–1826.

Sarret G, Willems G, Isaure MP, Marcus MA, Fakra SC, Frérot H, Pairis S, Geoffroy N, Manceau A, Saumitou-Laprade P. 2009. Zinc distribution and speciation in *Arabidopsis halleri* × *Arabidopsis lyrata* progenies presenting various zinc accumulation capacities. *New Phytologist* **184**: 581–595.

Scholl RL, May ST, Ware DH. 2000. Seed and molecular resources for Arabidopsis. *Plant Physiology* **124**: 1477–1480.

Shahzad Z, Gosti F, Frérot H, Lacombe E, Roosens N, Saumitou-Laprade P, Berthomieu P. 2010. The five AhMTP1 zinc transporters undergo different evolutionary fates towards adaptive evolution to zinc tolerance in *Arabidopsis halleri*. *PLoS Genetics* **6**: e1000911.

Szymanski DB, Jilk RA, Pollock SM, Marks MD. 1998. Control of *GL2* expression in Arabidopsis leaves and trichomes. *Development* **125**: 1161–1171.

Talke IN, Hanikenne M, Krämer U. 2006. Zinc-dependent global transcriptional control, transcriptional deregulation, and higher gene copy number for genes in metal homeostasis of the hyperaccumulator *Arabidopsis halleri*. *Plant Physiology* **142**: 148–167.

Thévenin J, Dubos C, Xu W, Le Gourrierec J, Kelemen Z, Charlot F, Nogué F, Lepiniec L, Dubreucq B. 2012. A new system for fast and quantitative analysis of heterologous gene expression in plants. *New Phytologist* **193**: 504–512.

Tremousaygue D, Manevski A, Bardet C, Lescure N, Lescure B. 1999. Plant interstitial telomere motifs participate in the control of gene expression in root meristems. *Plant Journal* **20**: 553–561.

Tuomainen M, Tervahauta A, Hassinen V, Schat H, Koistinen KM, Lehesranta S, Rantalainen K, Häyrinen J, Auriola S, Anttonen M *et al.* 2010. Proteomics of *Thlaspi caerulescens* accessions and an inter-accession cross segregating for zinc accumulation. *Journal of Experimental Botany* **61**: 1075–1087.

Verbruggen N, Hanikenne M, Clemens S. 2013. A more complete picture of metal hyperaccumulation through next-generation sequencing technologies. *Frontiers in Plant Science* **4**: 388.

Verbruggen N, Hermans C, Schat H. 2009. Molecular mechanisms of metal hyperaccumulation in plants. *New Phytologist* **181**: 759–776.

Visioli G, Pirondini A, Malcevschi A, Marmiroli N. 2010. Comparison of protein variations in *Thlaspi caerulescens* populations from metalliferous and non-metalliferous soils. *International Journal of Phytoremediation* **12**: 805–819.

Wang E, Gan S, Wagner GJ. 2002. Isolation and characterization of the *CYP71D16* trichome-specific promoter from *Nicotiana tabacum* L. *Journal of Experimental Botany* **53**: 1891–1897.

Wang S, Wang JW, Yu N, Li CH, Luo B, Gou JY, Wang LJ, Chen XY. 2004. Control of plant trichome development by a cotton fiber MYB gene. *Plant Cell* **16**: 2323–2334.

Weber M, Harada E, Vess C, von Roepenack-Lahaye E, Clemens S. 2004. Comparative microarray analysis of *Arabidopsis thaliana* and *Arabidopsis halleri* roots identifies nicotianamine synthase, a ZIP transporter and other genes as potential metal hyperaccumulation factors. *Plant Journal* **37**: 269–281.

Willems G, Dräger DB, Courbot M, Godé C, Verbruggen N, Saumitou-Laprade P. 2007. The genetic basis of zinc tolerance in the metallophyte *Arabidopsis halleri* ssp. *halleri* (Brassicaceae): an analysis of quantitative trait loci. *Genetics* **176**: 659–674.

Willems G, Frérot H, Gennen J, Salis P, Saumitou-Laprade P, Verbruggen N. 2010. Quantitative trait loci analysis of mineral element concentrations in an *Arabidopsis halleri*× *Arabidopsis lyrata petraea* F_2 progeny grown on cadmium-contaminated soil. *New Phytologist* **187**: 368–379.

Won SK, Lee YJ, Lee HY, Heo YK, Cho M, Cho HT. 2009. *Cis*-element- and transcriptome-based screening of root hair-specific genes and their functional characterization in Arabidopsis. *Plant Physiology* **150**: 1459–1473.

Yamamoto YY, Yoshitsugu T, Sakurai T, Seki M, Shinozaki K, Obokata J. 2009. Heterogeneity of Arabidopsis core promoters revealed by high-density TSS analysis. *Plant Journal* **60**: 350–362.

van der Zaal BJ, Neuteboom LW, Pinas JE, Chardonnens AN, Schat H, Verkleij JAC, Hooykaas PJJ. 1999. Overexpression of a novel Arabidopsis gene related to putative zinc-transporter genes from animals can lead to enhanced zinc resistance and accumulation. *Plant Physiology* **119**: 1047–1055.

Zhao FJ, Lombi E, Breedon T, McGrath SP. 2000. Zinc hyperaccumulation and cellular distribution in *Arabidopsis halleri*. *Plant, Cell & Environment* **23**: 507–514.

New Phytologist

Supporting Information

Additional Supporting Information may be found online in the Supporting Information tab for this article:

Fig. S1 ClustalW alignment of the *Arabidopsis halleri MTP1* promoters amplified from the ecotype I16 (in red), compared to the promoters of the population Auby as reported by Shahzad *et al.* (2010) (in black).

Fig. S2 Expression levels of the four *MTP1* sequences analysed by real-time RT-PCR on leaves of *Arabidopsis halleri* I16 plants grown in standard conditions.

Fig. S3 Qualitative GUS assay on leaf trichomes of 3-wk-old *Arabidopsis thaliana* plants transformed with the wild-type pAhMTP1-γ promoter and the mut155 promoter mutated in one MYB-binding site.

Fig. S4 Position of conserved motifs found by MEME analysis in the *MTP1* promoters of the different Brassicaceae species.

Table S1 Conservation among *MTP1* promoter sequences α, β and γ amplified from *Arabidopsis halleri* I16 and the *MTP1* promoters from *Arabidopsis thaliana, Arabidopsis lyrata* and *A. halleri* Auby, resulting from pairwise alignments

Table S2 List of the main *cis*-regulatory elements found in the *Arabidopsis thaliana, Arabidopsis lyrata* and *Arabidopsis halleri MTP1* promoters by PLACE analysis

Table S3 List of genes involved in metal tolerance and accumulation, whose promoter sequences were screened for MYB-binding motifs (CTGTTG)

Table S4 List of significant motifs found by MEME analysis in the *MTP1* promoters of different Brassicaceae species and their annotation in the PLACE database

Methods S1 *Arabidopsis thaliana* transformation.

Methods S2 Bioinformatic analysis of *MTP1* promoters.

Methods S3 Analysis of GUS and MTP1expression in transgeniclines.

Methods S4 Environmental scanning electron microscopy coupled with energy-dispersive X-ray spectroscopy (ESEM-EDS).

Please note: Wiley Blackwell are not responsible for the content or functionality of any Supporting Information supplied by the authors. Any queries (other than missing material) should be directed to the *New Phytologist* Central Office.